NASA/CR—2008-215236

Intelligent Engine Systems

Thermal Management and Advanced Cooling

Robert Bergholz
General Electric Aircraft Engines, Cincinnati, Ohio

June 2008

NASA STI Program . . . in Profile

Since its founding, NASA has been dedicated to the advancement of aeronautics and space science. The NASA Scientific and Technical Information (STI) program plays a key part in helping NASA maintain this important role.

The NASA STI Program operates under the auspices of the Agency Chief Information Officer. It collects, organizes, provides for archiving, and disseminates NASA's STI. The NASA STI program provides access to the NASA Aeronautics and Space Database and its public interface, the NASA Technical Reports Server, thus providing one of the largest collections of aeronautical and space science STI in the world. Results are published in both non-NASA channels and by NASA in the NASA STI Report Series, which includes the following report types:

- TECHNICAL PUBLICATION. Reports of completed research or a major significant phase of research that present the results of NASA programs and include extensive data or theoretical analysis. Includes compilations of significant scientific and technical data and information deemed to be of continuing reference value. NASA counterpart of peer-reviewed formal professional papers but has less stringent limitations on manuscript length and extent of graphic presentations.

- TECHNICAL MEMORANDUM. Scientific and technical findings that are preliminary or of specialized interest, e.g., quick release reports, working papers, and bibliographies that contain minimal annotation. Does not contain extensive analysis.

- CONTRACTOR REPORT. Scientific and technical findings by NASA-sponsored contractors and grantees.

- CONFERENCE PUBLICATION. Collected papers from scientific and technical conferences, symposia, seminars, or other meetings sponsored or cosponsored by NASA.

- SPECIAL PUBLICATION. Scientific, technical, or historical information from NASA programs, projects, and missions, often concerned with subjects having substantial public interest.

- TECHNICAL TRANSLATION. English-language translations of foreign scientific and technical material pertinent to NASA's mission.

Specialized services also include creating custom thesauri, building customized databases, organizing and publishing research results.

For more information about the NASA STI program, see the following:

- Access the NASA STI program home page at *http://www.sti.nasa.gov*

- E-mail your question via the Internet to *help@sti.nasa.gov*

- Fax your question to the NASA STI Help Desk at 301–621–0134

- Telephone the NASA STI Help Desk at 301–621–0390

- Write to:
  NASA Center for AeroSpace Information (CASI)
  7115 Standard Drive
  Hanover, MD 21076–1320

NASA/CR—2008-215236

Intelligent Engine Systems

Thermal Management and Advanced Cooling

Robert Bergholz
General Electric Aircraft Engines, Cincinnati, Ohio

Prepared under Contract NAS3–01135, Work element 4.2, Task order 37

National Aeronautics and
Space Administration

Glenn Research Center
Cleveland, Ohio 44135

June 2008

This work was sponsored by the Fundamental Aeronautics Program at the NASA Glenn Research Center.

Level of Review: This material has been technically reviewed by NASA technical management.

Available from

NASA Center for Aerospace Information
7115 Standard Drive
Hanover, MD 21076–1320

National Technical Information Service
5285 Port Royal Road
Springfield, VA 22161

Available electronically at http://gltrs.grc.nasa.gov

Intelligent Engine Systems
Thermal Management and Advanced Cooling

Robert Bergholz
General Electric Aircraft Engines
Cincinnati, Ohio 45215

Background

Turbine cooling accounts for 25% - 30% of core engine flow in modern commercial and military aircraft engines. Also, turbine airfoils (blades and vanes) constitute the majority of high-distress engine components limiting both commercial and military engine reliability. Efficient utilization and control of turbine cooling flows are essential for achieving high-efficiency engine cycles and minimizing combustor emissions. Reduction in cooling flows can reduce core size for a given thrust level and support the design of higher efficiency combustors. On the other hand, low-emission combustor designs generally produce flatter temperature profiles that can adversely impact current turbine cooling designs. Hence, turbine cooling technology has been identified under Propulsion 21 as a critical element for continued development of advanced gas turbine engines.

Objective & Approach

The objective is to provide turbine-cooling technologies to meet Propulsion 21 goals related to engine fuel burn, emissions, safety, and reliability. Specifically, the GE Aviation (GEA) Advanced Turbine Cooling and Thermal Management program seeks to develop advanced cooling and flow distribution methods for HP turbines, while achieving a substantial reduction in total cooling flow and assuring acceptable turbine component safety and reliability. Enhanced cooling techniques, such as fluidic devices, controlled-vortex cooling, and directed impingement jets, offer the opportunity to incorporate both active and passive schemes. Coolant heat transfer enhancement also can be achieved from advanced designs that incorporate multi-disciplinary optimization of external film and internal cooling passage geometry.

Task 4.2.1 TMS Concepts, Component Design and Fabrication (GE Aviation)

Subtask 4.2.1.1 3D HPT Blade Inverse Cooling Design and Optimization

The turbine airfoil cooling designer is faced with a variety of choices for internal cooling methods and geometries. One approach to the selection of internal cooling features is to apply "inverse design" techniques. This process is best developed as a concept evaluation or preliminary design tool, but is important to retain the full 3D external aerodynamic and heat transfer distributions to achieve a reasonable level of accuracy in the analysis and allow for a first-level optimization of cooling flow and

The procedure developed here uses a "zonal" approach to modeling the airfoil cooling. 3D CFD results for static pressure, temperature, and heat transfer coefficients are mapped on a "shell" model of the airfoil. The airfoil shell is discretized into cooling zones, with the external heat loads and sink pressures defined by the local 3D CFD mapping. The internal (backside) cooling for each zone is free to be defined by the designer, e.g., near-wall convection, convection with turbulators, impingement, film holes, etc.. The zones are inter-connected in the model by inflows and outflows of coolant. These flows are driven by pressure differences between zones, or between the zone and the local external sink pressure in the case of a zone with film holes. Film flow emanating from a zone is tracked via the 3D streamlines from the CFD solution.

An example of a discretized airfoil with the 3D CFD mappings of pressure, temperature, and heat transfer coefficients is shown in the following figure.

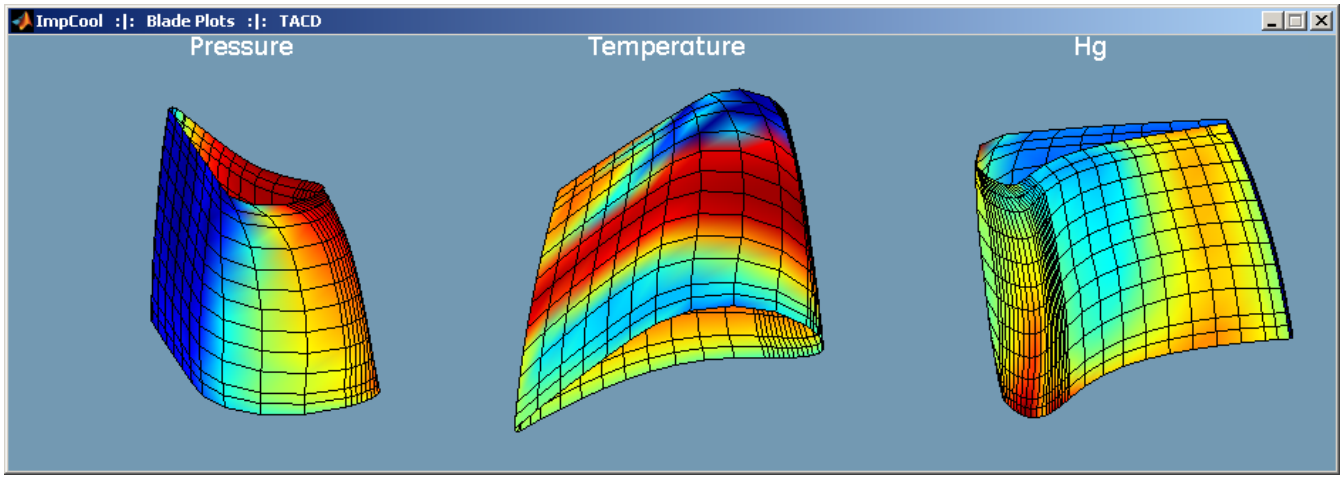

Figure 4.2.1.1.1 Airfoil shell zonal model

The procedure is implemented in MATLAB. An example of the primary design input screen is shown in the following figure.

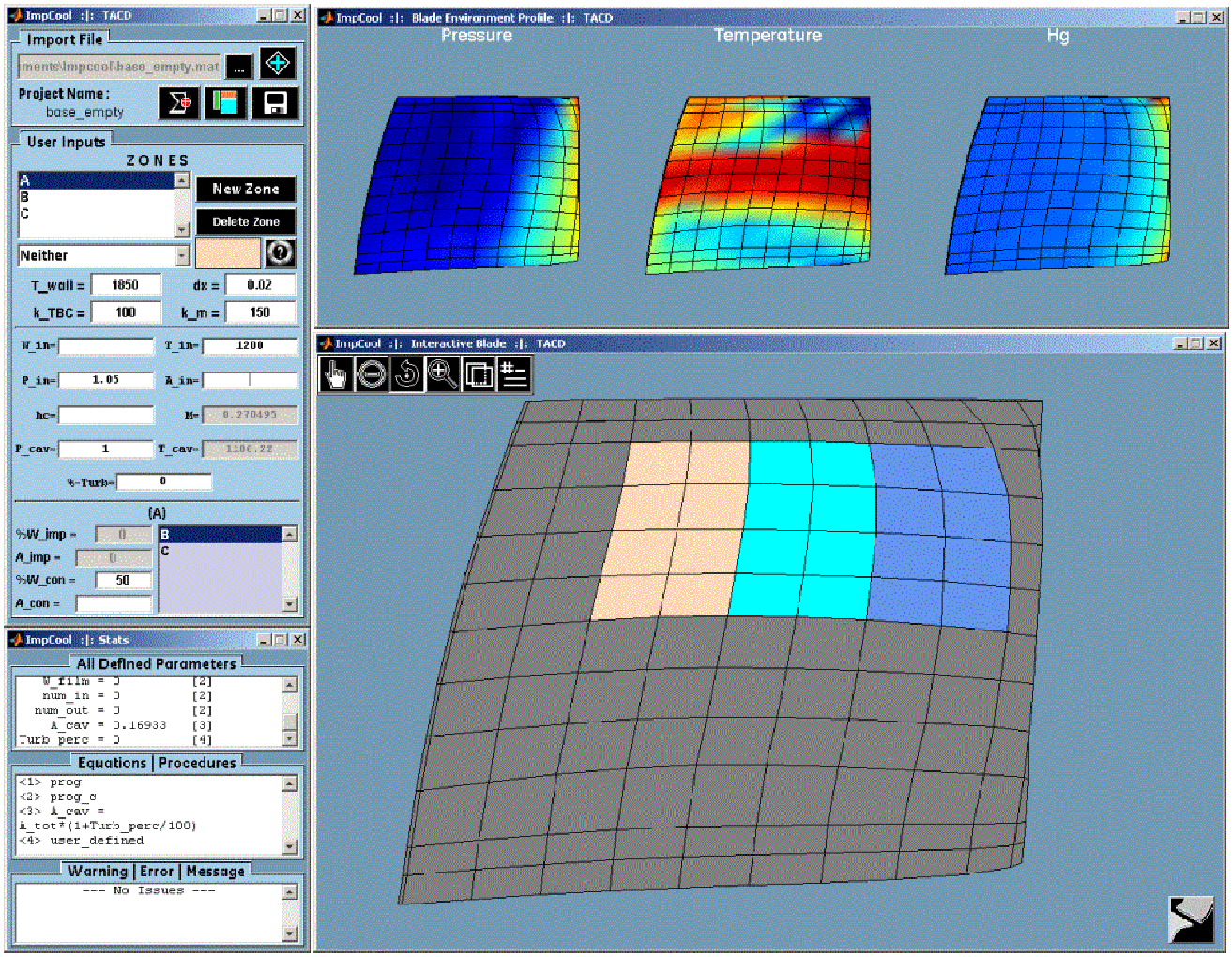

Figure 4.2.1.1.2 MATLAB Cooling Model Interface

The following discussion gives some of the key details of the process and describes the overall structure of the model. The procedure is illustrated for four cooling combination, but other are also possible.

Having the knowledge of how much flow, for a given cooling method, is required in a particular region of a turbine blade allows the engineer to budget the total available cooling flow to achieve the required amount of cooling throughout the blade. It is possible to back-solve for various properties in a cooling system, given appropriate models/correlations, so as to accomplish heat transfer and continuity equilibrium. A system is described in both the heat transfer/thermodynamic and flow/continuity realms. The fundamental flow/continuity equations:

$$\dot{m} = \rho \cdot V \cdot A \Rightarrow \rho \cdot (M \cdot a) \cdot A \Rightarrow \rho \cdot \left(M \cdot \sqrt{\gamma \cdot R \cdot T_s}\right) \cdot A \Rightarrow \left(\frac{P_s}{R \cdot T_s}\right) \cdot \left(M \cdot \sqrt{\gamma \cdot R \cdot T_s}\right) \cdot A$$

$$\frac{T_t}{T_s} = 1 + \left(\frac{\gamma - 1}{2}\right) \cdot M^2 \quad \Big| \quad \frac{P_t}{P_s} = \left(\frac{T_t}{T_s}\right)^{\left\langle \frac{\gamma}{\gamma - 1} \right\rangle} \quad \Big| \quad \frac{P_t}{P_s} = \left[1 + \left(\frac{\gamma - 1}{2}\right) \cdot M^2\right]^{\left\langle \frac{\gamma}{\gamma - 1} \right\rangle}$$

$$\dot{m} = \left(\frac{P_t}{\sqrt{R \cdot T_t}}\right) \cdot A \cdot \sqrt{\gamma} \cdot M \cdot \left[1 + \left(\frac{\gamma - 1}{2}\right) \cdot M^2\right]^{\left\langle \frac{\gamma + 1}{2 - 2\gamma} \right\rangle}$$

Along with the fundamental thermodynamic/heat transfer equations:

$$\dot{Q} \equiv k_{therm} \cdot \left(\frac{A_M}{\Delta x}\right) \cdot \Delta T \equiv h_{therm} \cdot A_M \cdot \Delta T \equiv \dot{m} \cdot c_p \cdot \Delta T \equiv \dot{m} \cdot \Delta h$$

$$\mathrm{Re} = \frac{W_{imp} \cdot di \cdot T_{jet}}{A_{imp} \cdot \mu \cdot T_{fimp}} \quad \Big| \quad T_{fimp} = \frac{T_{jet} +_M T_{II}}{2}$$

$$\mathrm{Pr} = \frac{\mu \cdot c_p}{k_{therm}} \quad \Big| \quad Nu_{avg} = f(\mathrm{Re}, s/d, z/d, \mathrm{Pr})$$

The governing equations can be coupled and manipulated to allow for the solution of various parameters, given limited information. For instance, to achieve a desired maximum surface temperature while given pressure ratio and coolant temperature (in addition to other material and environment properties/boundary conditions) for the case of impingement cooling, the coolant flowrate can be inversely calculated to achieve that target maximum temperature. That newly discovered flowrate is what balances the governing equations for the given information.

To use this concept on a broader scale and application, the Impcool Design Utility was developed - with the aid of MATLAB - to allow for the visualization and preliminary design of turbine cooling systems. It uses a system of governing equations (those expressed on the first page) to model various cooling methods in order to solve for any possible ***unknown*** parameters given any particular set of ***known*** parameters. The broader aspect of this application is that it allows for the designing of various ***types*** of cooling methods:

1. ***Impingement & Film***
   + Incoming mass flow : external source and/or different (conjoined) system(s)
   + Outgoing mass flow : film row (optionally, conjoined system(s))
2. ***Impingement without Film***
   + Incoming mass flow : external source and/or different (conjoined) system(s)

+ Outgoing mass flow : conjoined system(s)

3. ***Film without Impingement***
   + Incoming mass flow : external source and/or different (conjoined) system(s)
   + Outgoing mass flow : film row (optionally, conjoined system(s))
4. ***Convective*** (neither impingement nor film)
   + Incoming mass flow : external source and/or different (conjoined) system(s)
   + Outgoing mass flow : conjoined system(s)

The governing equations for these four key methods of cooling can be developed into individual systems of equations from which the various parameters of respective cooling methods can be determined. When the cooling methods are interconnected, they represent a unique flow configuration between various regions/zones of the blade whose parameters are inter-related among the respective ***types*** of cooling.

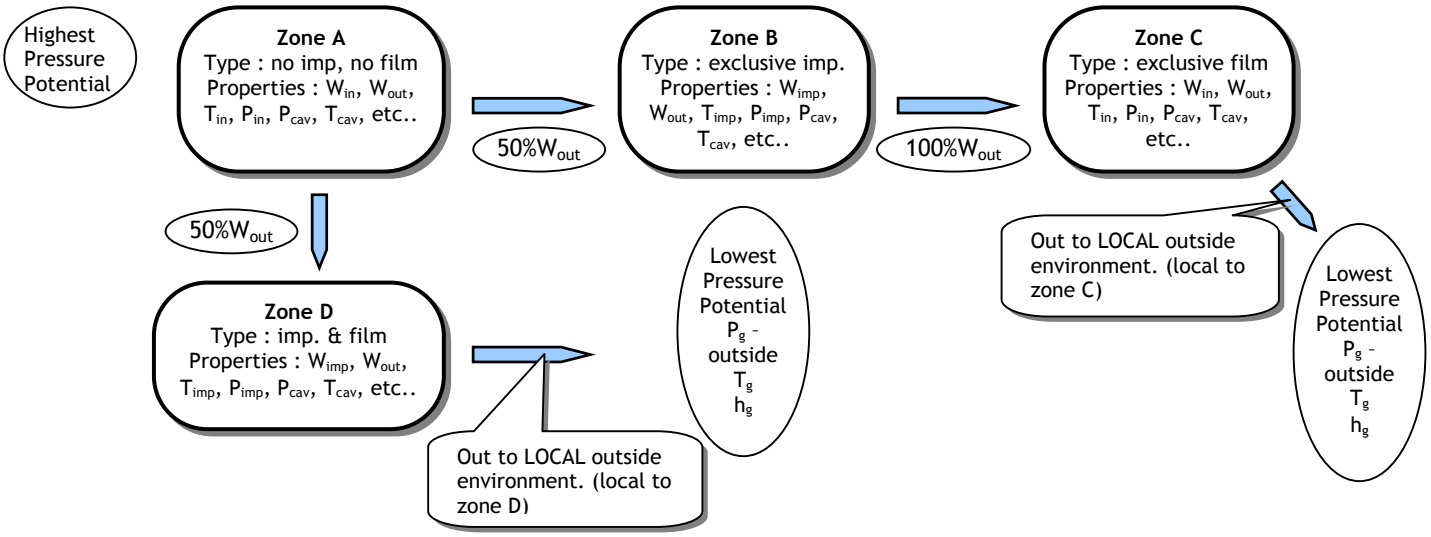

Figure 4.2.1.1.3 : Sample schematic of blade cooling configuration

The zones of these configurations are in a constant state of check between one another so as to adhere to the governing rules of continuity (flow function). When a parameter of any zone within a configuration is modified (added/removed/changed), the entire configuration is updated to meet the continuity requirements for that configuration. Each zone within a configuration is interrogated to "understand" its upstream and downstream environment.

Once the zone's parameter is modified (for instance, zone B), the solver looks for all the incoming (zone A) and outgoing (zone C) flows associated with that zone (zone B). If there are any incoming or outgoing flows, the flow properties of those zones (if available) are used to update the other parameters of the zone in question (zone B). Otherwise, the current zone (zone B) determines whether it should/could update any parameters in either the upstream (zone A) or downstream (zone C) zones. At the heart of the solver is the ability to sift through the governing equations and, using all of the currently known variables/parameters, solve for any other possible variable(s). If any new parameters are in

fact found, the current zone – along with its upstream and downstream constituents – are updated to reflect the new discovery.

Given the fact that some of the cooling methods create an external film layer on the blade, there is a need for preliminary processing between zone types for recognition of such zones with respect to any other zones that may be affected by the exiting film. For instance, if a particular zone utilizes a film cooling method, all immediate downstream (stream-wise) zones are affected –to some degree- by the exiting film of the initial film-type zone. The film effectiveness produced –for subsequent downstream zones- is modeled to be exponentially decreasing as a function of the distance from the initial film exit to the location of those downstream zones.

The goal of such a utility is to be able to design the overall cooling system of a turbine blade while taking into account the effects of different methods of cooling on one another (taking into account the effects and conditions of different regions of the blade) while managing the total available cooling flow.

Impingement & Film Method

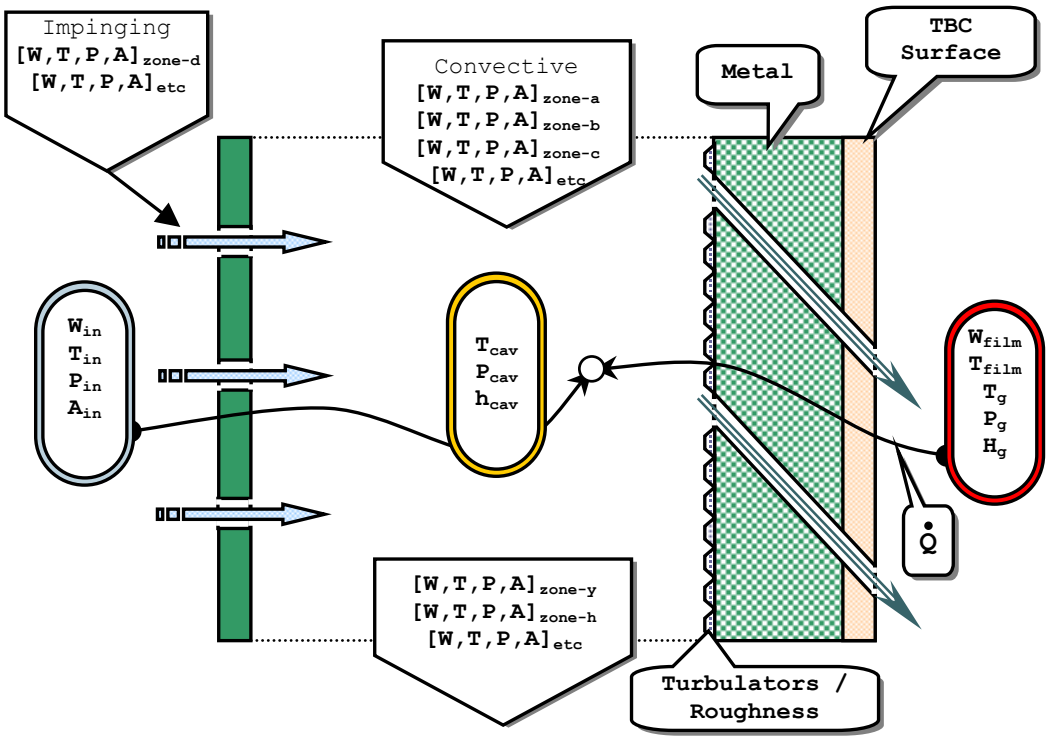

Figure 4.2.1.1.4 : Architecture for impingement cooling with film exit

The current model for calculating the effects of impingement for this type of cooling method (as depicted in Figure 4.2.1.1.4) is an algerbraic correlation. It makes use of the average

Nusselt number as modified by the geometric constraints of the system to determine the effective heat transfer coefficient due to impingement.

$$Nu = Nu_{avg} \cdot \chi = \frac{h_c \cdot di}{k_{therm}}$$

Due to the natural diffusivity of the impinging jet – as it exits the impingement orifice - the algebraic correlation for an arrayed impingement system is limited with respect to the offset distance from when the jet exits the impingement wall (orifice) to when it makes contact with the hot wall (metal surface).

The air that is impinged upon the hot wall in this method can be utilized in several ways. Initial cooling occurs at impingement, while the air can be treated over the hot wall via impingement bumps or surface roughness to enhance the heat transfer from hot wall to coolant. The air is then expelled through film holes to the outside environment where the blade's outside surface is cooled by the exiting film layer. Optionally, the air can be bled to different zones of the blade to provide secondary internal cooling.

Impingement Without Film Method

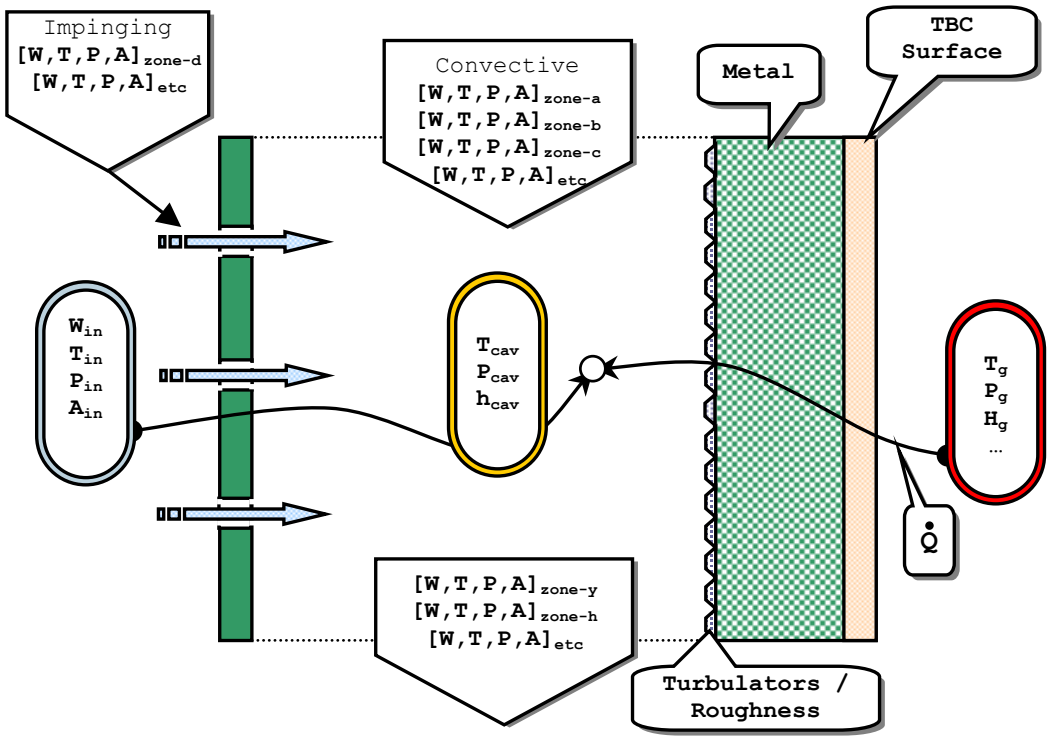

Figure 4.2.1.1.5 : Architecture for impingement cooling without film exit

This method is similar to that of the previous method (Impingement with Film exit), with the exception of a film exit. The total amount of flow going into such a zone must exit via

connective bleeds to other zones. The algerbraic Nu correlation is again used to find the heat transfer coefficient due to impingement as an average for the total (h) for the cavity between the impingement wall and hot wall (metal surface). Since the mass flow through the impingement wall is connected to the heat transfer quantity, the required amount of flow can be determined for a given amount of heat pickup through the blade. This mass flow is used to size the impingement holes for a given pressure ratio, operating condition.

$$\dot{m} = \left(\frac{P_t \cdot A_{imp}}{\sqrt{R \cdot T_t \cdot (\gamma - 1)}} \right) \cdot \sqrt{2\gamma \cdot \left[\left(\frac{P_t}{P_s} \right)^{\left\langle \frac{\gamma-1}{\gamma} \right\rangle} - 1 \right] \cdot \left(\frac{P_t}{P_s} \right)^{\left\langle \frac{\gamma+1}{2\gamma} \right\rangle}}$$

$$A_{hole} = \frac{A_{imp}}{nhi} = \left(\frac{\pi}{4} \right) \cdot di^2 \Rightarrow di = \sqrt{\frac{4 \cdot A_{imp}}{\pi \cdot nhi}}$$

By these means, the engineer can determine how to place the impingement holes for optimal cooling – either by increasing the number of holes and decreasing the impingement hole size or increasing the hole size while decreasing the number of holes. Previous analytical results tell us that smaller impingement holes achieve a more favorable result for cooling.

Film Without Impingement Method

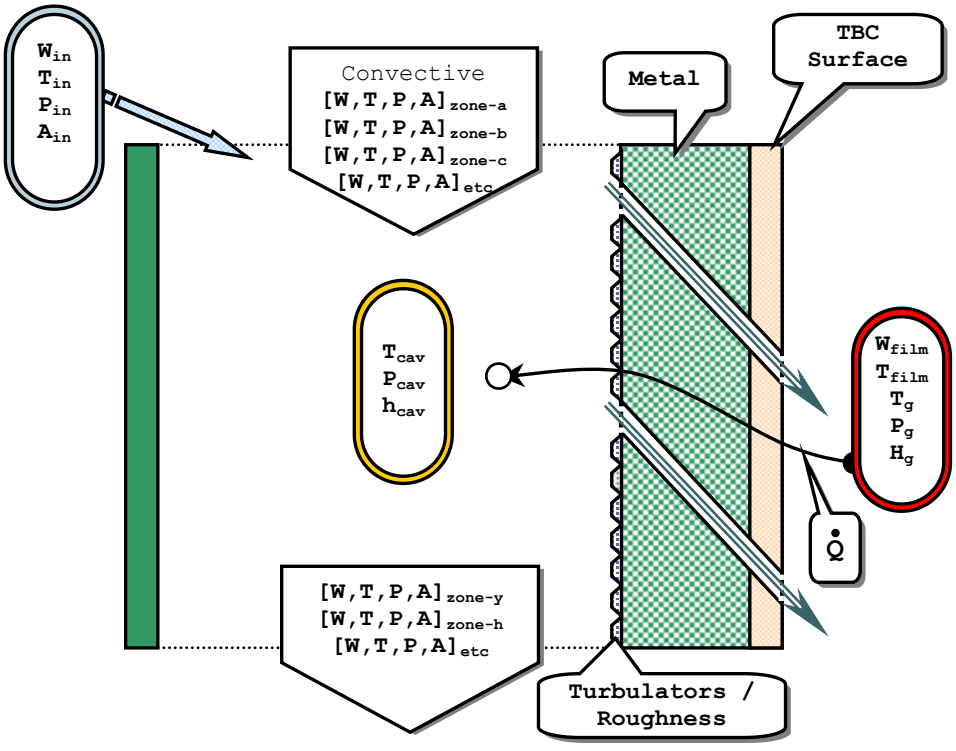

Figure 4.2.1.1.6 : Architecture for film cooling without impingement

The cavity heat transfer coefficient for this sort of cooling method is determined not by means of the impingement correlation, rather by conventional duct heat transfer methods. The incoming air (coolant) absorbs heat from the wall - which may have an enhanced heat transfer surface area for better/fuller conductivity – while it exits through film holes in the wall from which it may further absorb heat from the metal. The film of air expelled is then used to cool the downstream blade surface – much like the previously described method of impingement with film exit.

Much like the technique used for determining the impingement hole size in the previous cooling method, given the heat transfer and pressure ratio between the environment and blade cavity, the film hole size can be determined by coupling the continuity equation with the heat transfer equation system for convective and duct flow (that being through the film holes).

Convective Method

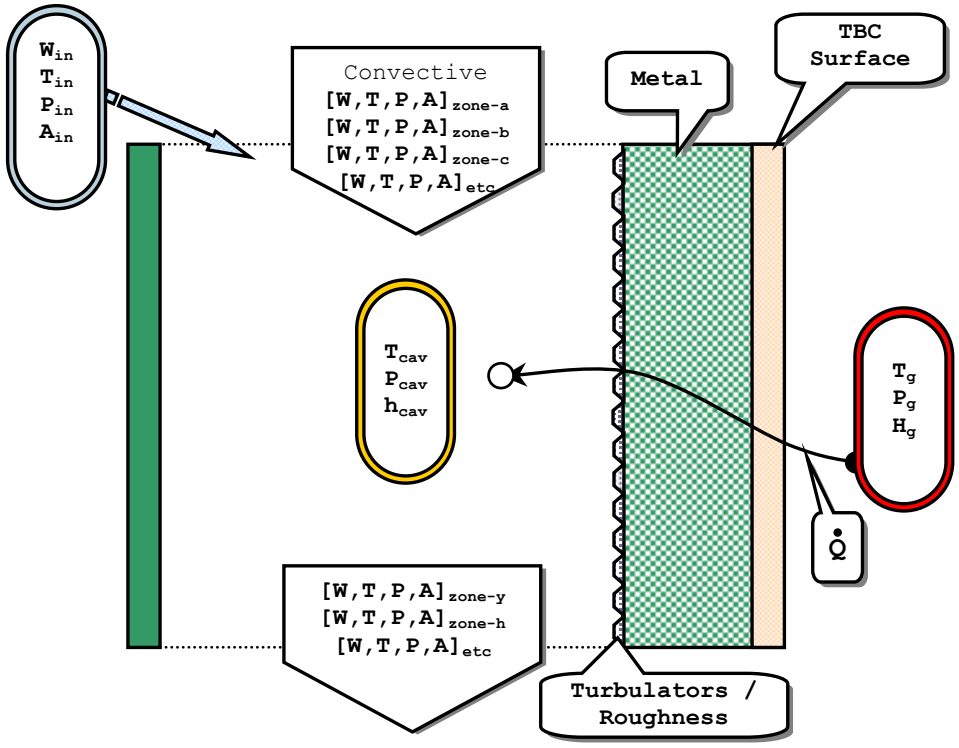

Figure 4.2.1.1.7 : Architecture for cooling without impingement or film exit (near-wall)

The simplest of the four cooling methods used in this program is the case of purely convective heat transfer – that being without impingement or film exit. The incoming airflow is treated over the hot wall (metal) to absorb heat (optionally, with the assistance of surface enhancement features like turbulators or surface roughness). This method of cooling is depictive of current near-wall cooling passages used in turbine blades. The air is then bleed to other zones for secondary cooling purposes.

It can be seen that the generic heat transfer and continuity equations hold true for this and the other methods of cooling. The primary difference between these methods is the way the air is utilized for such cooling; this lends itself to a systematic method for determining appropriate cooling configurations on a larger scope with interconnected cooling systems – as in the cooling system of an entire blade.

ImpCool Design Utility

This application utilizes equations/correlations/models as defined by the user/engineer to generate a solution for the various methods of cooling. In its database, it contains a default set of governing equations for the four methods of cooling along with a default set of correlations for global/universal variables like air, metal, and heat capacity properties. These equations, in effect – the way the solver works, are entirely controlled by the user. The concept of this application is to allow the engineer to model the cooling methods so as to represent the most current techniques used for solving such problems.

Features

+ *Save/Open projects* : After creating the various cooling configurations with the design utility, the user/engineer may want to save the information/configuration in order to come back at a later time to update or improve the model.
+ *Auto log generation* : This feature of the application works in the background to keep track of what the user has done with the utility just in case something goes wrong and information is lost; the user can look at the history of the lost project to recreate the cooling model(s)/configuration(s).
+ *Inline program/solver diagnostics* : This feature notifies the user whenever there is a program (or solver) related constrain/error and tries to counteract the issue automatically (if possible). A solver related constraint might have something to do with how the user sets up the cooling configurations or the governing equations (which may interfere with one another or cause other program/solver related errors).
+ *Equation editor for adding/removing/modifying governing equations* : This feature allows the user/engineer to modified the governing equations to better suit the type of cooling system the engineer is trying to achieve. The ImpCool Design Utility comes with a default set of modeling equations hard-coded, ready for any modifications.
+ *Equation variable combination generator* : This feature takes care of the mundane task of multiple term/equation creation when modifying equations; it is used when the user wants to generate equations for all terms within a particular equation, so that each term has a chance to be solved.
+ *Skin Thickness Distribution Designer (STDD)* : This feature allows the engineer to modify the blade's metal thickness by entering either the exact desired thickness or percent augmentation for the selected region(s).

+ *Report Generator* : This feature generates an excel file containing all information about the designed cooling system; it also generates PowerPoint slides of the blade environment maps (BC profiles) and the interactive blade configurations created by the user.

Solver Architecture

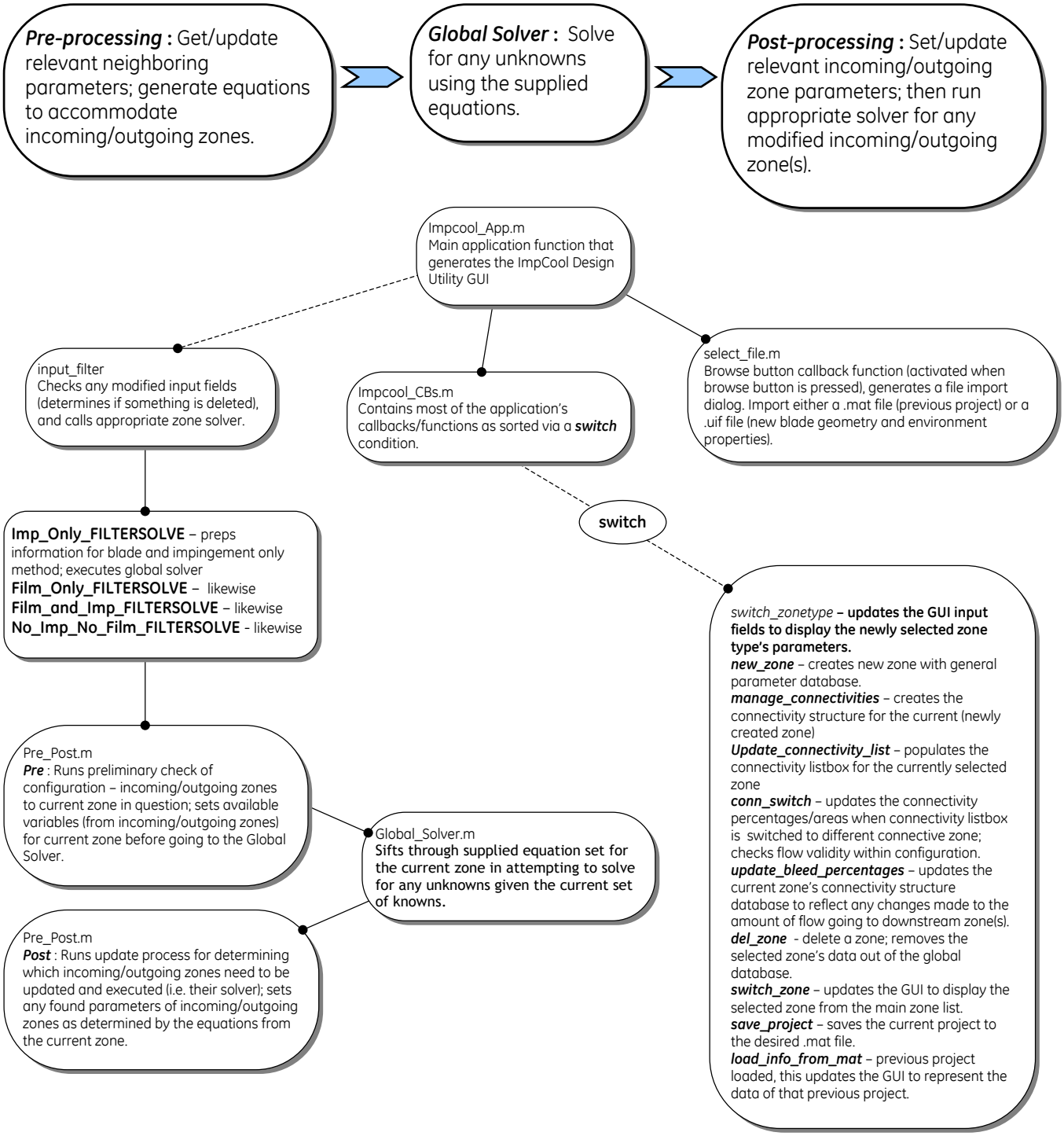

Subtask 4.2.1.2 Impingement Cooling Modeling and Optimization

Background

Impingement cooling is an important element in many turbine airfoil cooling designs. Impingement cooling performance is governed by several parameters, among them jet Reynolds number, impingement pressure ratio, the impingement hole pitch to diameter ratio, and the impingement gap to hole diameter ratio. The goal is to minimize the impingement cooling flow for a given heat transfer area and external heat load.

Objectives

The first objective of this study is to model impingement cooling in sufficient detail to allow optimization of the impingement geometry to minimize the required cooling flow for a target maximum metal temperature. The second objective is to develop a impingement heat transfer model to predict the local impingement heat transfer coefficient distribution for an arbitrary array of staggered or in-line impingement holes. The local heat transfer coefficient distributions can then be applied to prediction of the local variation of metal temperatures. This is especially important for sparse impingement arrays for which there is a significant variation in local heat transfer coefficient.

Technical Approach

MATLAB models were developed for the impingement flow minimization process and for the prediction of local impingement heat transfer coefficients. A generalized impingement cooling correlation used for the flow minimization procedure. The local impingement heat transfer coefficient distribution was simulated by an analytical equation that captures the impingement jet stagnation point behavior and allows correlation to experimental data through adjustable constants.

Results

Minimization of Impingement Cooling Flow for Target Twall and Given Heat Load

The impingement flow minimization model in illustrated by a simple example of a turbine airfoil surface subject to a specified distributions of external gas temperature and heat transfer coefficient. The external wall of the airfoil is broken into arbitrary zones of given external heat transfer area, Hgas, and Tgas. Each zone is modeled as an individual impingement region with a amount of cooling flow and hole pattern to be determined by the impingement optimization procedure. This is illustrated in Figures 4.2.1.2.1 and 4.2.1.2.2.

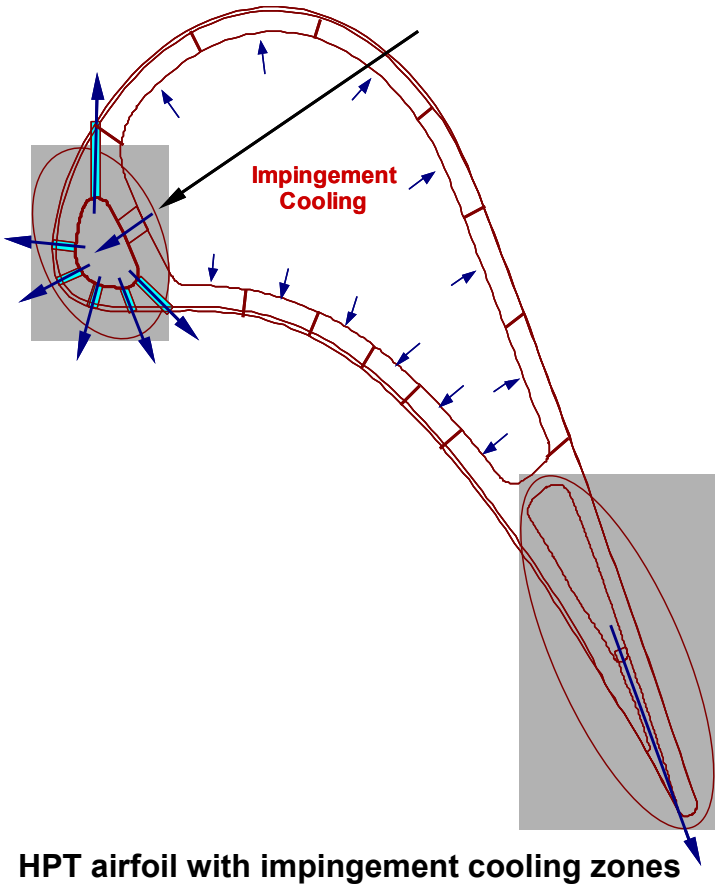

Figure 4.2.1.2.1 HPT airfoil with impingement cooling zones

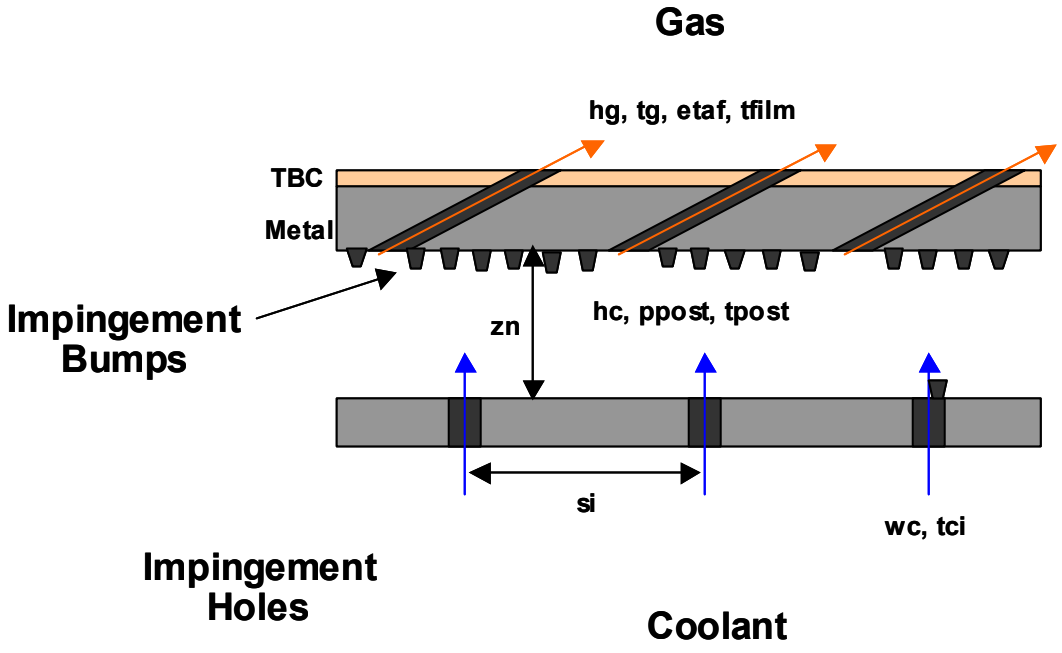

Figure 4.2.1.2.2: Zonal impingement cooling model

The external hot-gas heat transfer coefficient and temperature conditions are show in Figure 4.2.1.2.3.

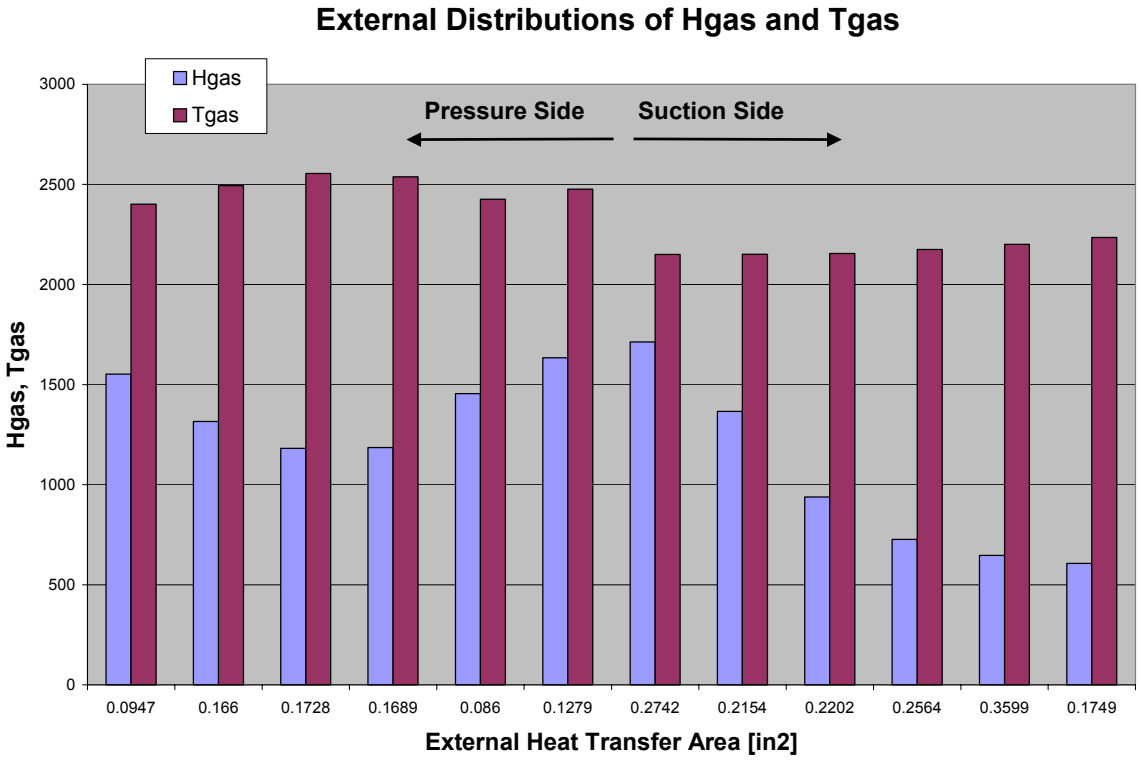

Figure 4.2.1.2.3: External Hgas and Tgas distributions.

A target wall temperature distribution is specified for the interface between the TBC and the base metal. The impingement cooling model then iterates to minimize the required impingement cooling flow for each zone. The resulting cooling flow distribution is shown in Figure 4.2.1.2.4 and the wall temperatures are shown in Figure 4.2.1.2.5.

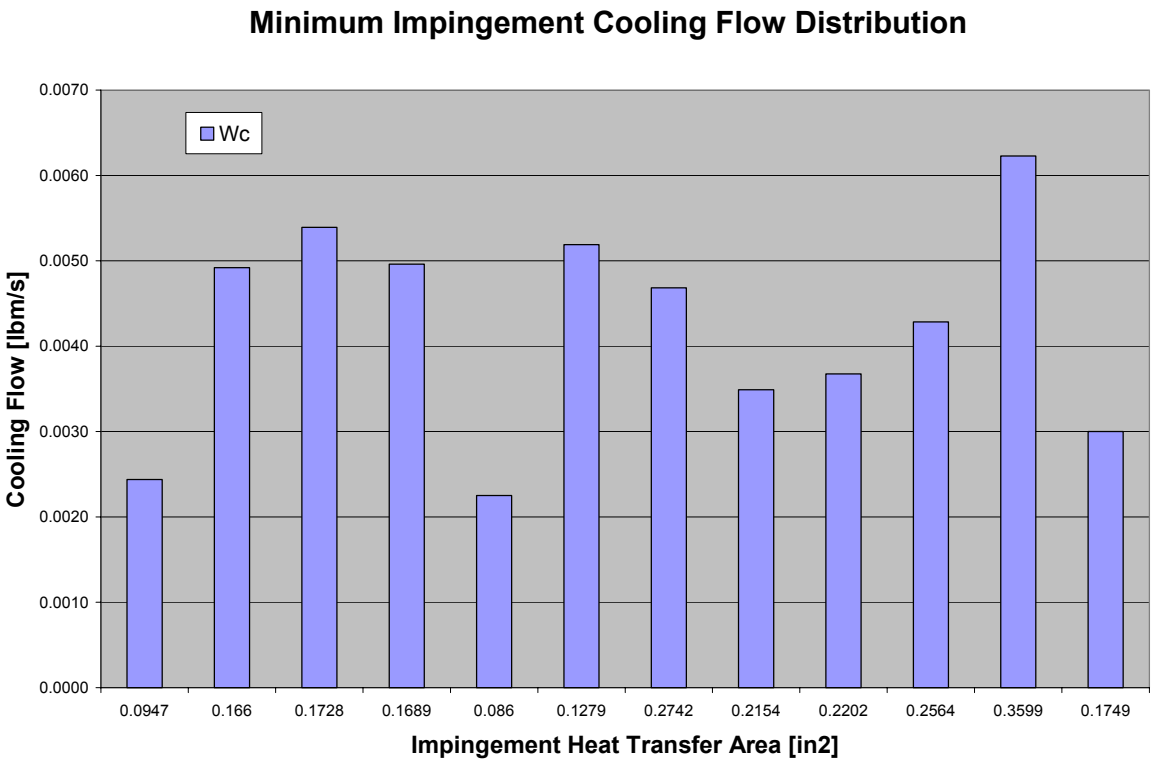

Figure 4.2.1.2.4: Distribution of minimum impingement cooling flow.

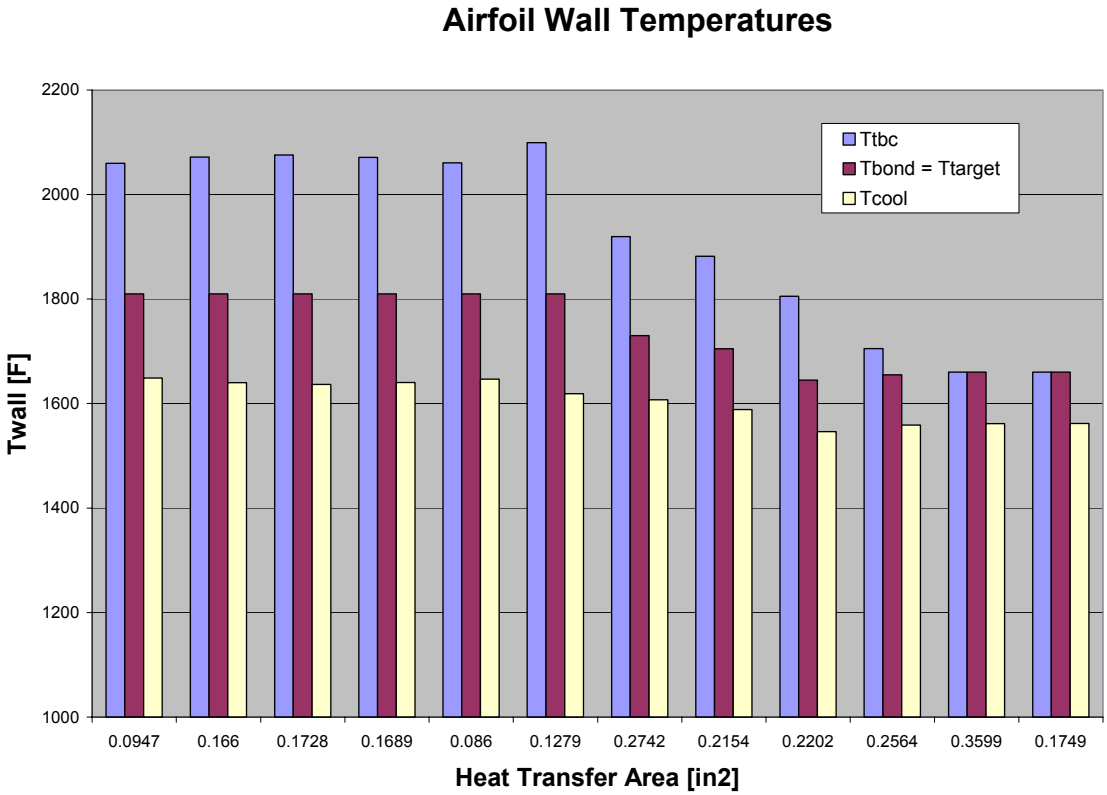

Figure 4.2.1.2.4: TBC and metal temperature distributions.

Local Impingement Heat Transfer Coefficient Model

A local multi-hole impingement heat transfer coefficient model was constructed from a simplified algebraic expression for a single jet, as follows.

$$hc = C(x) \cdot \exp(-\sigma(\theta) * r^{\alpha})$$

The resulting local impingement heat transfer coefficient distribution is illustrated for a 3 x 6 in-line impingement hole array in Figure 4.2.1.2.5.

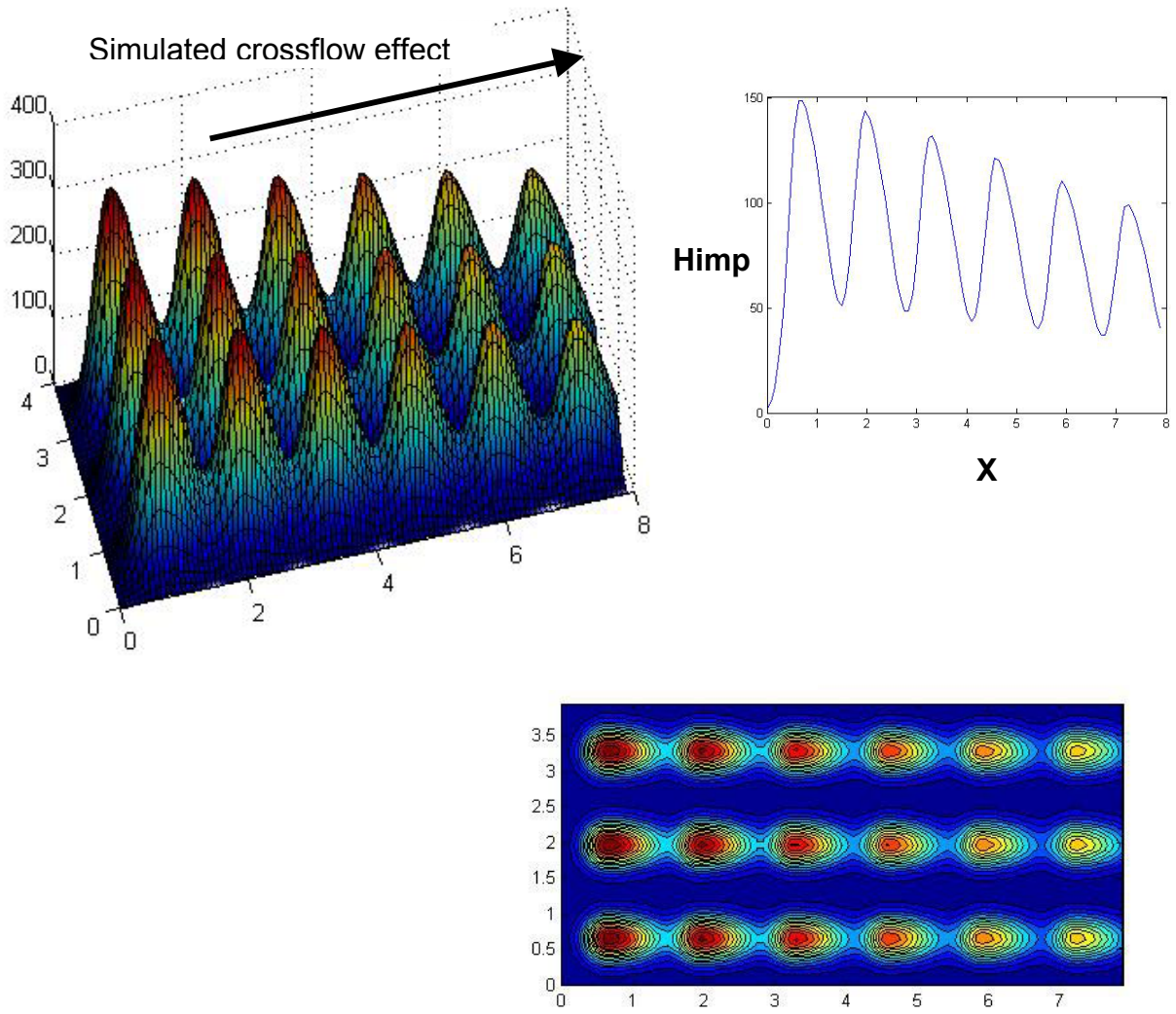

Figure 4.2.1.2.5: Local Himp model - 3 x 6 array

The effect of local impingement heat transfer coefficient variation for a relatively sparse staggered array of impingement holes is shown in Figure 4.2.1.2.6. The resulting temperature gradients in the plane of the wall can lead to undesirable thermal stresses. Future work will extend the optimization process to minimization of maximum temperature and thermal gradients for a specified cooling flow distribution.

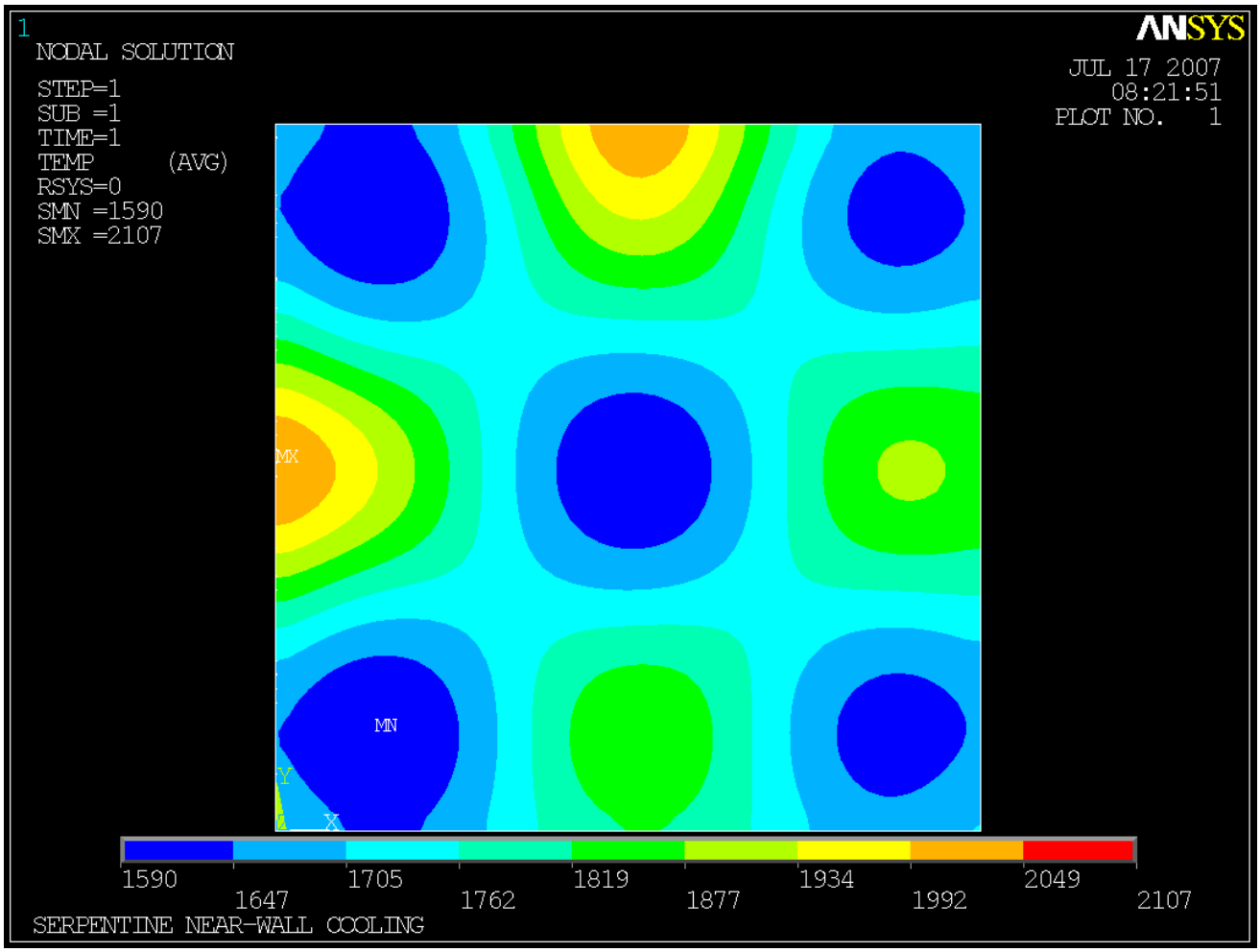

Figure 4.2.1.2.6: Wall temperature distribution induced by sparse impingement array.

Conclusions

The impingement cooling optimization process discussed above can be incorporated into the full 3D blade cooling optimization process discussed in Subsection 4.2.1.1.

Subtask 4.2.1.3 Vortex Valve Performance Tests

Background

An aircraft engine experiences different conditions during its flight mission. During takeoff and climb, the engine is generating the most power and its hot section parts, especially in the high-pressure turbine, are experiencing the most severe thermal conditions. The mainstream temperature and flow is at its maximum level and the cooling flow temperature also is at its maximum level. Later, during the cruise part of the mission at high altitude, the temperature and flow levels are lower, reducing the heat flux through the hot section components. Historically, the cooling flow delivery to the high-pressure turbine rotor has been sized for the severe takeoff and climb conditions. This flow level is usually much higher than required to cool the turbine at the cruise condition. This reduces the engine's efficiency during the performance-critical cruise portion of the mission. Previous efforts to introduce valves to control the cooling flow delivered to the HP turbine have not succeeded because of the mechanical complexity of the proposed system -- the design community is very reluctant to rely on mechanical-actuated components on a mission-critical part of the design such as the HP turbine cooling flow.

A new control valve has been proposed that does not rely on mechanically actuated components. Instead, the valve design is static, i.e., it does not have any moving parts. The flow through the valve is controlled in two ways: 1) the relative difference in thermal growth of valve components fabricated from different materials and 2) a vortex swirl introduced inside the valve to lower the pressure leaving the valve.

Objectives

A test program was run to obtain flow data to support the design of the new vortex valve. Pressure and flow measurements were needed to determine the flow function performance characteristics for a proposed vortex valve design.

Technical Approach

A sketch of the test model used in the test is shown in Figure 4.3.1.3.1 and a photograph of the model is shown in Figure 4.3.1.3.2. The test model did not directly model the thermal growth attributes of the proposed design, but permitted testing of the thermal growth effect through the insertion of washers between the adjustable piston and the fixed shaft at the centerline of the valve. The flow through the valve is partially controlled by changes in flow area caused by shifting of the adjustable piston. Additional control is provided by a swirl vortex produced by a pair of swirl jets introduced at 180^{o} opposing locations in the gap between the piston and the outer wall of the valve.

Flow was introduced into the test model through the ports indicated on the left side of Figure 4.3.1.3.1 and exited out of the single port on the right side of the model. A portion of the flow is bled out of the plenum and reintroduced through two swirl jets inside the model,

simulating the proposed engine application. Additional tests were run with an independent swirl jet supply. Pressure measurements were taken at a number of locations inside the model.

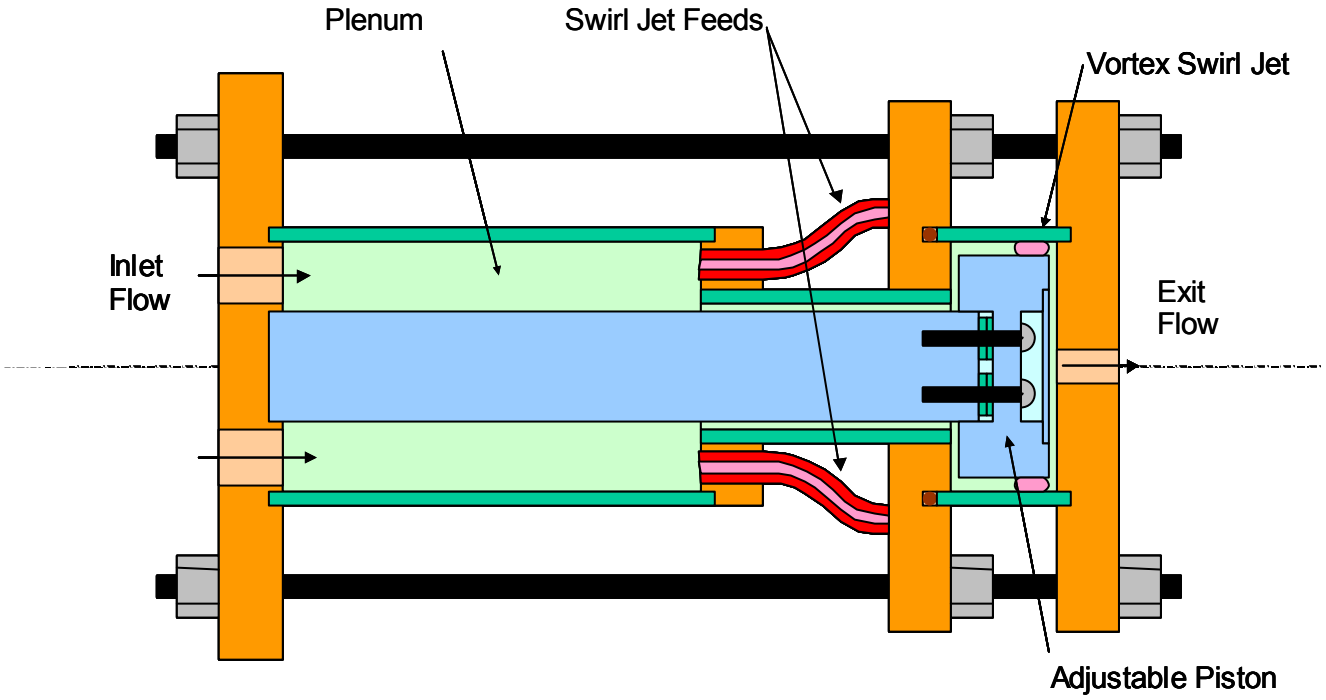

Figure 4.3.1.3.1 Sketch of Cross-Section of Vortex Valve

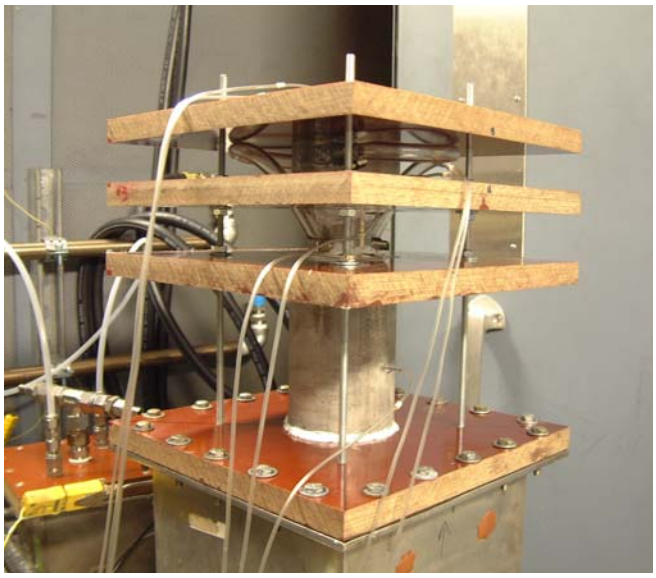

Figure 4.3.1.3.2 Photograph of Vortex Valve Test Model

Results

Additional GE Proprietary details about the test, including dimensional information about the design of the vortex valve and tabulated flow and pressure results, may be obtained from the author.

Conclusions

Flow data was obtained on a model of a vortex valve design that has been proposed for regulating the turbine coolant flow. The results obtained with the vortex valve were forwarded to the design group responsible for the coolant flow system design.

Subtask 4.2.1.4 Cooling Flow Modulation

A passive, pressure-actuated cooling flow modulation device was studied, again using MATLAB as the modeling tool. A typical hydro-formed bellows was modeled as a spring acted on by pressure and deflection forces. The bellows is assumed to be attached to an aerodynamically shaped, axially translating element (plug) inside a contoured orifice (see example below).

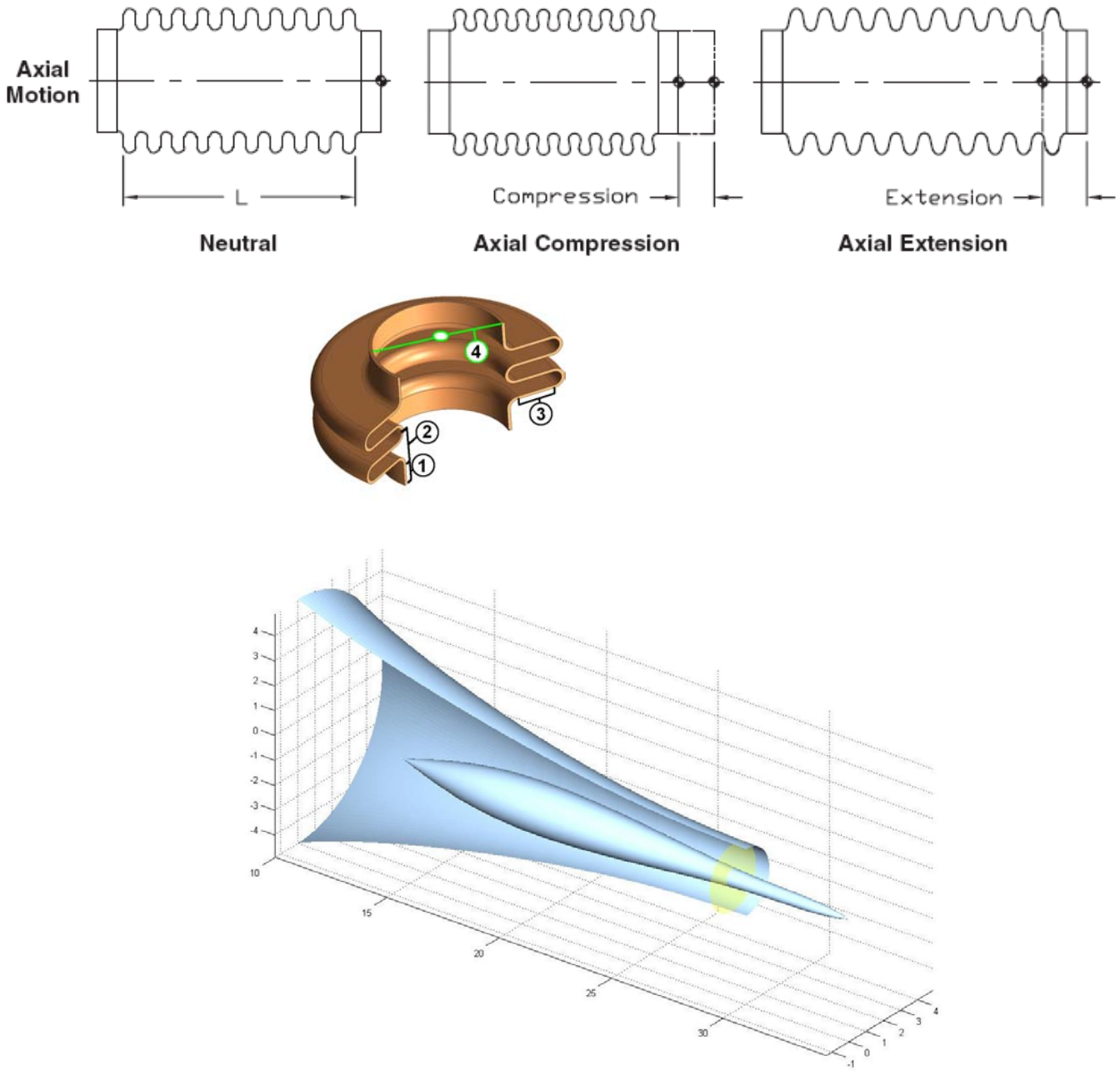

Figure 4.2.1.4.1 Pressure-actuated bellows flow control device

The MATLAB model interface screen below. The model can compute the orifice throat area, and hence the flow, for any axial location of the plug. This device was shown to effectively control flow while maintaining low total pressure losses.

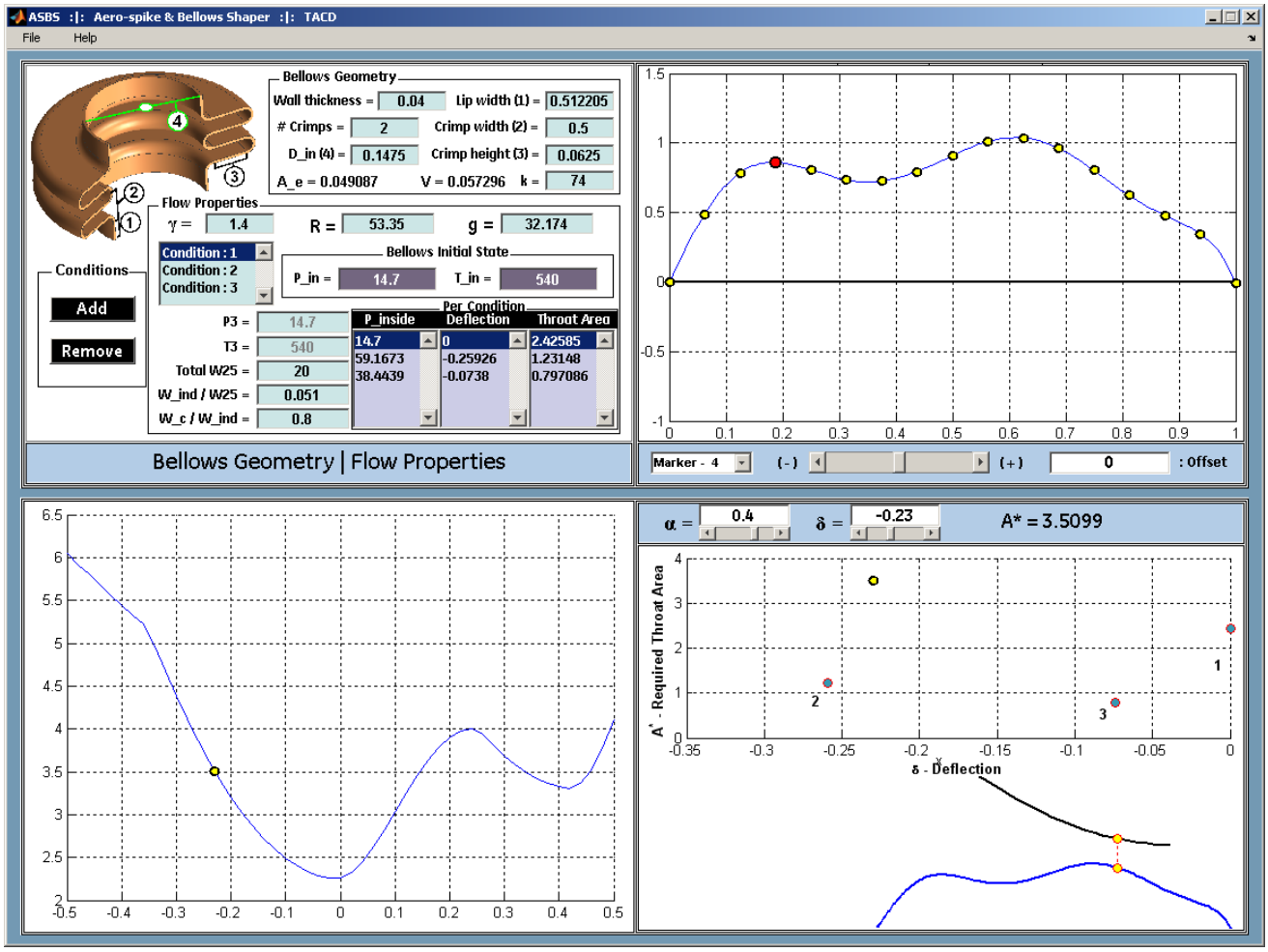

Figure 4.2.1.4.2 MATLAB flow modulation device design interface

Task 4.2.2 Advanced Cooling Feature Technologies and Testing

Computational and experimental studies were performed to test enhanced cooling features relevant to stage 1 gas turbine blades. Detailed CFD analysis was performed for a variety of trailing edge slot configurations. The CFD was post processed and compared in terms of non-dimensional performance parameters (described later). The non-dimensional performance parameters provide a means of comparing each slot configuration's performance on a global basis.

Impingement heat transfer studies were also performed both computationally and experimentally. Various surface features placed on a target plate, including chevrons and vortex generators, were analyzed. The goal was to assess whether various features provided benefit in terms of heat transfer or pressure drop performance. Configurations *without* surface features were also analyzed. These experiments provided surface maps of heat transfer coefficients for sparse impingement arrays. As with the trailing edge slot studies, global performance metrics were also evaluated.

Subtask 4.2.2.1 Trailing Edge Cooling CFD Modeling

Background & Objectives
A high aspect ratio channel, typical of a trailing edge cavity in a stage 1 blade, was identified for CFD analysis. Several concepts were suggested by GE-Aviation for evaluation. CFD simulations were performed to predict the relative performance of the different designs with respect to coolant heat pick up and pressure drop. The objective was to investigate performance for novel geometric configurations likely to induce greater mixing and greater streamwise vorticity.

Technical Approach
The high aspect ratio channel was constrained to a cavity with a 16-degree wedge angle (8 degree half angle). Realistic cavity aspect ratios, fillets, etc were used. Figure 4.2.2.1 shows the baseline cross-section.

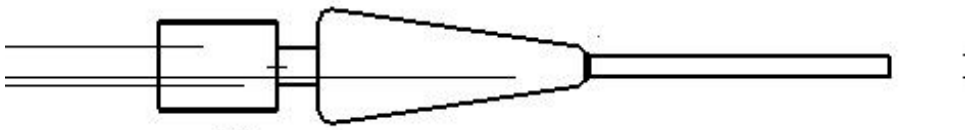

Figure 4.2.2.1 Cross-section of baseline configuration.

Coolant was supplied to the cavity through a channel emulating a crossover impingement hole. A supply feed volume was used such that *vena contracta* effects through the crossover hole were captured. The coolant was then exhausted through a channel that emulates a trailing edge slot. Symmetry boundary conditions were imposed so that one pitch was modeled.

CFD simulations were completed for several different configurations. Descriptions of the configurations are given in below.

(a) This configuration is the baseline configuration where the inlet and exit of the coolant into and from the cavity are coaxial.
(b) This configuration is a variation of (a) where the inlet has been shifted laterally off center.
(c) This configuration is a variation of (a) where the inlet has been angled 45 degrees in the lateral plane, with the opening of the inlet channel (crossover hole) in the cavity is aligned coaxially with the exit channel.
(d) This configuration is a variation of (c) where the inlet channel has been shifted vertically by half a pitch.
(e) This configuration is a variation of (a) where a post obstruction has been placed laterally across the cavity and normal to the exit channel axis.
(f) This configuration is a variation of (c) where a row of 10 bumps or pins has been placed on the side opposite of inlet jet impingement.
(g) This configuration is a variation of (c) where a second inlet channel has been modeled and angled 45 degrees in the other direction from center than the first inlet

channel, creating a symmetric cell of a vertical series of jets at alternating angles of +-45 degrees.

Simulations were performed using an SST turbulence model. This turbulence model was chosen mostly because it lends itself to wall integration and is less prone to the stagnation point heat transfer anomaly.

Results

The results of these configurations were evaluated to compare relative performance. The best solution is design specific and is not necessarily the one with the highest overall average Nusselt number. The coolant has a finite cooling capacity. As it passes through the cavity and slot, it must retain enough cooling capacity to maintain the surrounding metal temperatures within allowable levels. The temperature through the slots must also be of an appropriate magnitude to provide adequate film cooling effectiveness on trailing edge lands after the slot breakout. For these models, the slot breakout is not modeled.

Although one configuration cannot be deemed superior to another, a summary table has been created that shows each configuration's respective performance. The table, included in the GE proprietary version on this report, summarizes the following parameters:

- Total temperature rise across the computational domain (inlet to exit)
- Total pressure loss across the circuit (inlet to exit)
- Normalized heat transfer coefficients broken down on a wall by wall basis
  - -PS- pressure side cavity wall
  - -SS- suction side cavity wall
  - -FWD- forward cavity wall
  - -AFT- aft cavity wall
  - -PSSLOT- pressure side wall of slot
  - -SSSLOT- suction side wall of slot
  - -SLOTTOP- top of slot
  - -FILLET- fillet of slot
- Relative heat pickup across the cavity and the slot
- Heat Sink Utilization
- Heat Transfer Rate over pumping power

The heat sink utilization is a measure of how much heat is transferred from the wall to the fluid divided by the maximum heat that could have been delivered assuming the coolant temperature eventually reaches the hot wall temperature. The heat sink utilization is defined as

$$\Sigma = \frac{\int q''dA}{\dot{m}Cp(Twall - Tinlet)}$$

The heat transfer rate divided by the pumping power is defined as

$$\Phi = \frac{\rho_{avg}\int q''dA}{\dot{m}\Delta P}$$

and is a measure of the amount of heat transfer relative to the amount of power required to drive the fluid from inlet to exit.

Subtask 4.2.2.2 Impingement Cooling CFD Modeling and Tests

Computational studies were performed for various impingement array configurations. Various surface features were placed on the impingement target plate and performance was assessed in terms of the global performance metrics discussed in Subtask 4.2.2.1

Experimental measurements were carried out for the various impingement array configurations as well as in combination with the turbulating features in order to assess the performance and validate CFD modeling.

CFD Modeling

Background & Objectives

An impingement hole orifice plate was selected as a baseline for CFD analysis. Several surface features were modeled on the target surface. Literature and experimental data is plentiful for surface features placed in duct flow type configurations. However, literature is sparse for surface features used in impingement flow regimes. As such, the goal was to investigate whether the inclusion of geometric features enhanced or degraded system performance.

Technical Approach

The impingement simulations consisted of an orifice plate with a rectangular array of holes. The rectangular array represented a relatively sparse impingement configuration where the hole to hole spacing was kept fixed at 10 jet diameters. The jet to target distance was kept fixed at 4.5 jet diameters. Three walls bounded the rectangular channel (the region between the jet issuing orifice plate and target plate). This allowed the flow to exhaust in only one direction and also allowed cross flow to be built up.

An upstream plenum was modeled which provided the flow to the orifice plate. The plenum was included such that vena contracta effects were captured. All walls were treated adiabatically with the exception of the impingement target surface. This surface was modeled as isothermal. The impingement jet to target wall temperature ratio was kept fixed at 0.75. An inlet mass flow condition was set in order to provide an average jet Reynolds number of 5000. On average, this corresponded to an overall pressure ratio (plenum total pressure to exhaust static pressure) of 1.05. Turbulence intensity was set to five percent and an eddy to molecular viscosity ratio of 10 was prescribed. As with the trailing edge slots

discussed in subtask 4.2.2.1, a wall integration approach using the SST turbulence model was used.

CFD simulations were completed for several different configurations. Descriptions of the configurations are given below.

(a) Smooth wall baseline- Represents the baseline impingement configuration without any surface geometry features placed on the target surface
(b) 90 Degree Ribs- This configuration is a variation of (a) where turbulators at an angle of attack of 90 degrees have been modeled on the target surface. The turbulators are placed between the impinging jets.
(c) Chevrons- This configuration is a variation of (a) where chevrons have been modeled on the target surface. The chevrons are placed between the impinging jets
(d) Ramps- This configuration is a variation of (a) where inclined ramps have been modeled on the target surface. The ramps are placed directly underneath the impinging jets
(e) Square Pedestals- This configuration is a variation of (a) where square pedestals have been modeled on the target surface. The pedestals are placed directly underneath the jets.
(f) Vortex generators- This configuration is a variation of (a) where vortex generators have been modeled on the target surface. The vortex generators are placed between the impinging jets.

Results

The relative performance of all configurations was assessed. As with the trailing edge slots discussed in subtask 4.2.2.1, the CFD results were post processed and global performance parameters were analyzed. A summary of this performance as well as local distributions of wall heat flux on the target surfaces are shown for the different impingement configurations in the companion version of this report that includes GE proprietary data..

Conclusions

It was anticipated that the different surface features would provide much larger differences in terms of overall performance metrics (as was seen in the trailing edge slot cfd studies). It is unfortunate that the cfd predictions yield rather consistent results for various surface features making it difficult to quantify whether any features behave profoundly different.

Impingement Cooling Tests

Background and Objectives

As mentioned earlier, there is plentiful of data found in the public domain on jet impingement. However, the data available in the public domain is usually for cases where Reynolds number, pressure ratio and spacing-over-diameter are confounded and result in incomplete data sets for correlations. Similarly, the public domain lacks studies with impingement in combination with flow modifying features, such as turbulators, are investigated for performance enhancement.

The objectives of this experimental effort are provide good data sets of heat transfer measurements for impingement cooling where the three parameters, Reynolds number, pressure ratio and spacing-over diameter, are unconfounded and therein provide a more comprehensive set of data for correlation and CFD validation purposes. Also, three flow-modifying features were investigated for potential heat transfer performance enhancement with minimal pressure loss generation.

Experimental Hardware Description

The experimental study involved a setup composed mainly of an upstream plenum, varying plates of arrays of impingement holes, a collecting channel and a downstream back-pressured plenum, Figure 4.2.2.5. The jets exiting the hole-array plates into the collecting channel impinged onto a target surface instrumented with a thin-foil heater and a sheet of wide-band liquid crystals, used for generating a constant heat flux condition and measuring temperatures respectively.

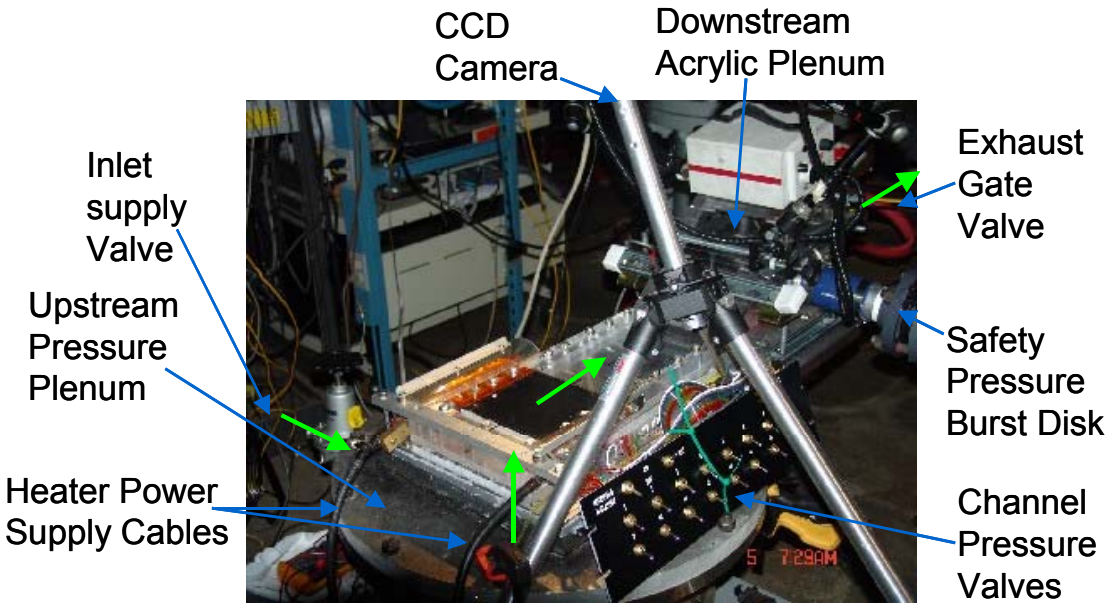

Figure 4.2.2.5 –Imping ment cooling rig with various components.

Pressure taps were machined onto the hole-array plates in-between holes for measuring static pressures. A control panel of pressure valve switches, connecting stabilizing manifolds to the pressure taps, allowed for individual measurement of pressures at the discrete locations in the channel. Figure 4.2.2.6 illustrates a zoomed-out view of experimental hardware.

Figure 4.2.2.6 – Zoomed-out view of Impingement cooling rig.

Figure 4.2.2.7 – Flow-modifying features investigated. From top to bottom, delta wings, chevrons and ramps.

The three flow-modifying features are illustrated in Figure 4.2.2.7. The delta wing and chevron features were positioned approximately 2 to 3 hole-diameters downstream of the

peak impingement location to act more as flow turbulators. The ramps were positioned in a manner such that the impinging jet centered near the top of the ramp, approximately 1 hole-diameter downstream from the front edge of the feature, and centered in the width portion of the feature. Different t to the delta wing and chevron features, the ramps acted more to distribute the impinging jet and presumable redirect some of the jet momentum downstream of the impingement location.

Technical Approach

As mentioned previously, liquid crystals were used to measure complete surface maps of temperatures on the target surface. Figure 4.2.2.8 illustrates a typical steady-state liquid crystal color map for one of the impingement cases tested. The liquid crystal data, in combination temperature measurements taken with discrete thermocouples and measurements of voltage and current passed through the foil heater to generate a constant heat flux condition, we used to compute heat transfer coefficient distributions for the variety cases considered.

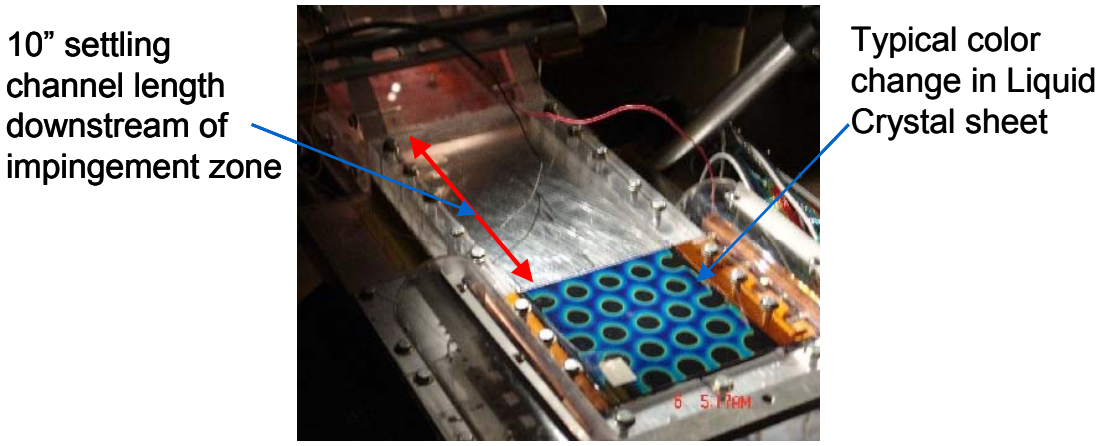

Figure 4.2.2.8 – Liquid crystal measurement of impingement jet array.

The convective heat flux was defined by,

$$q_{conv.} = q_{heater} - q_{cond.loss}$$

where the power produced by heater was computed by,

$$q_{heater} = \frac{V \times I}{A_{heater}}$$

and the conduction losses though the acrylic window were accounted for and computed by,

$$q_{cond.loss} = \frac{K_{acrylic} \times (T_{imp.surface} - T_{acrylicBS})}{A_{heater}}$$

Finally, the convective heat transfer coefficient was computed by,

$$h = \frac{q_{conv.}}{(T_{imp.surface} - T_{jet})}$$

where $T_{imp.surface}$ is the surface temperature measured by the liquid crystal, T_{jet} is temperature of the jet measured at the upstream plenum, V is the voltage input to the heater, I is the current input the heater, $K_{acrylic}$ is the thermal conductivity for Acrylic window and A_{heater} is the area of the heater.

Uncertainty analyses were carried out for each distribution map of heat transfer coefficients generated.

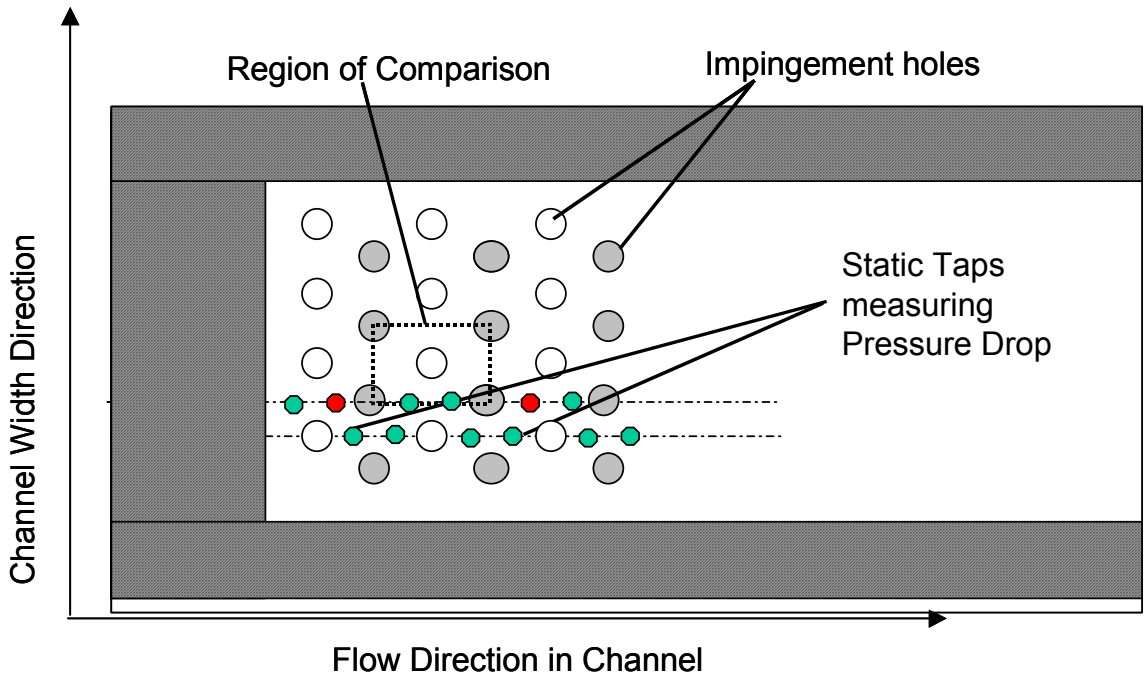

Figure 4.2.2.9 – Arrangement of static pressure taps for measuring pressure drop inside channel across region of comparison.

The arrangement and location of static pressure taps are illustrated in Figure 4.2.2.9. As depicted by the smaller circles filled with the green and red, two rows of pressure taps were machined to the side of the center region of comparison. The rows were purposefully placed there to avoid causing interference to the region of comparison, but also to avoid picking up an effects from the sidewalls. The circles in red were used to compute the

characteristic pressure drop for the individual tests. An inclined water manometer with 0.01inH20 resolution was used to measure the pressures by taking one of the taps as a reference. The pressure valve system used selecting individual pressure channels is shown in Figure 4.2.2.5.

Results

The liquid crystal data in combination with measurements made with thermocouples and measurements of voltage and current from the foil heater used were used to generate heat transfer coefficient maps for both smooth channel cases and turbulated channel cases. Figure 4.2.2.10 illustrates a complete map of heat transfer coefficients for typical case of impingement cooling test. In order to match both Reynolds number and pressure ratios for the different spacing-over-diameter (SOD) cases, variations in the holes sizes and the number of holes were made. For all cases considered, the region of comparison, as pointed out in Figure 4.2.2.10, was chosen to lie in the middle of the channel width-wise, and after the first row of impingement jets. This provided similar conditions between the varying geometries and avoided issues of sidewall effects. As delineated by the dashed-line enclosing rectangle, the region of comparison connects the center of four jet-impingement regions (clearly shown by the heat transfer distribution maps) and encloses the heat transfer coefficient distribution of one complete jet including its surrounding data. Distributions for only the region of comparison are presented and discussed. Similarly, averages and peaks are extracted from the data within the region of comparison.

Commonly seen in all results and as can be expected, as seen in Figure 4.2.2.10, the jets generate lower heat transfer coefficients further downstream in the channel as the channel flow accumulates. Similarly, the heat transfer signatures become less concentric and more skewed and tear-like further downstream.

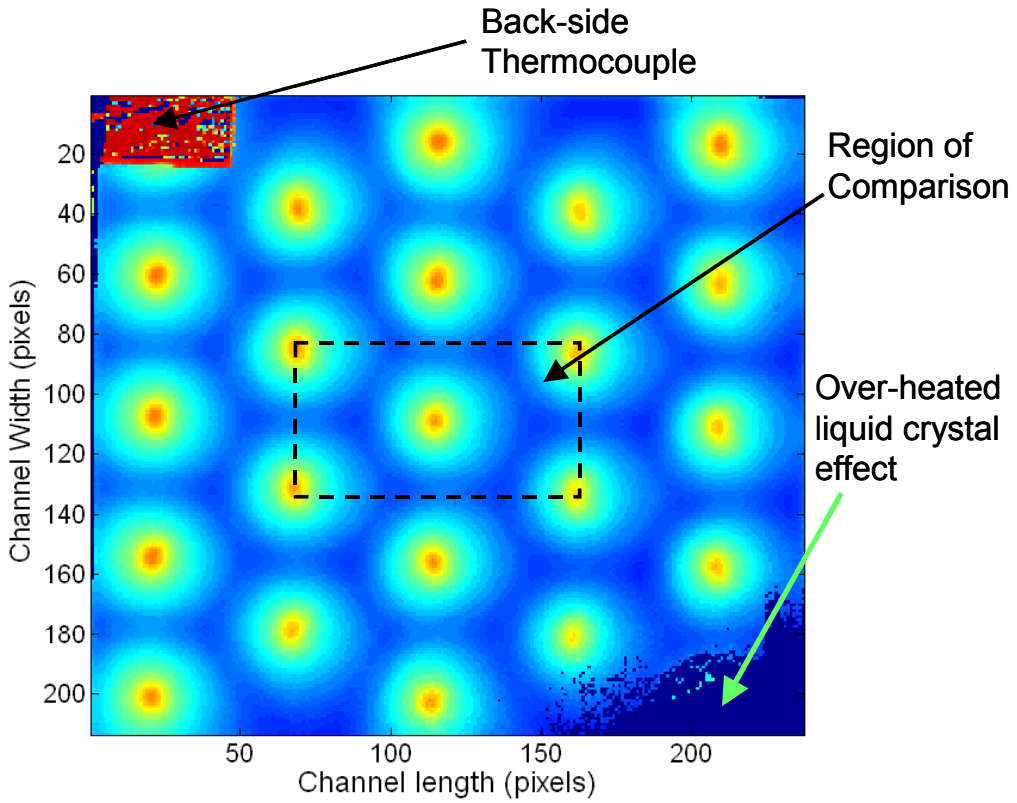

Figure 4.2.2.10 – Typical complete heat transfer coefficient map generated from liquid crystal experiment.

Smooth Channel

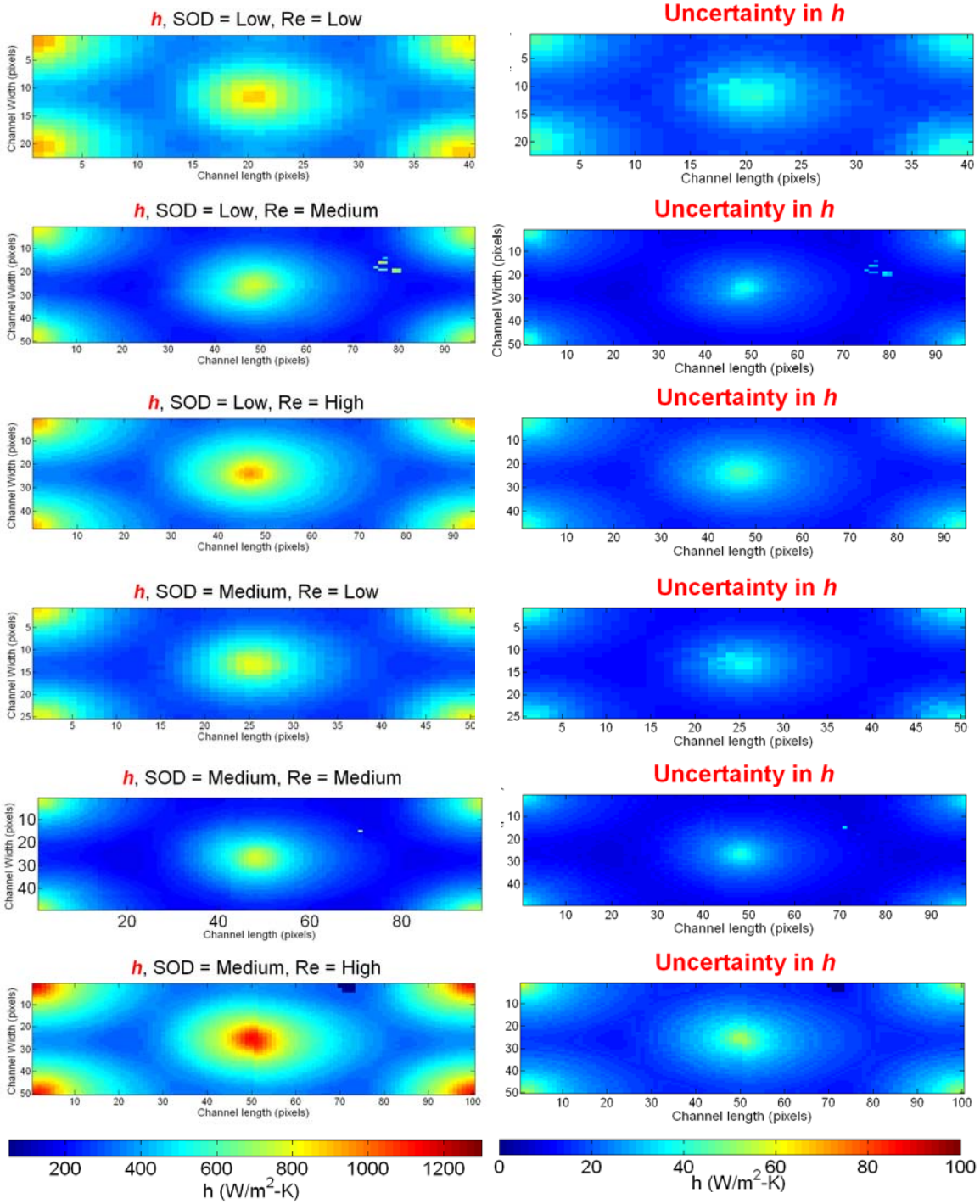

Figure 4.2.2.11 – Heat transfer distributions with associated uncertainty maps for varying flow conditions tested for SOD Low and SOD Medium. Note: color scale is common between ***h*** maps and Uncertainty in ***h*** maps, respectively.

Figure 4.2.2.11 presents the heat transfer coefficients for the low and medium SOD cases for the three Reynolds numbers at an approximately similar pressure ratio. Alongside, detailed maps of uncertainty in the heat transfer coefficient maps are also presented. The trend shows the higher heat transfer coefficients for the higher Reynolds number at for the same pressure ratio. As expected, heat transfer coefficient distributions are better for the higher Reynolds number, where the jet seems to disperse further out from the target center, in terms of both average and peak values. The two case for the middle Reynolds number cases require further looking in to as they do not follow the general increasing trend as expected. The questionable values are within the uncertainty of the experiment, but need further investigating. Potential causes are the different rigs used for these two cases in comparison to the other tests. Also, different heaters were used as well as different Acrylic thicknesses.

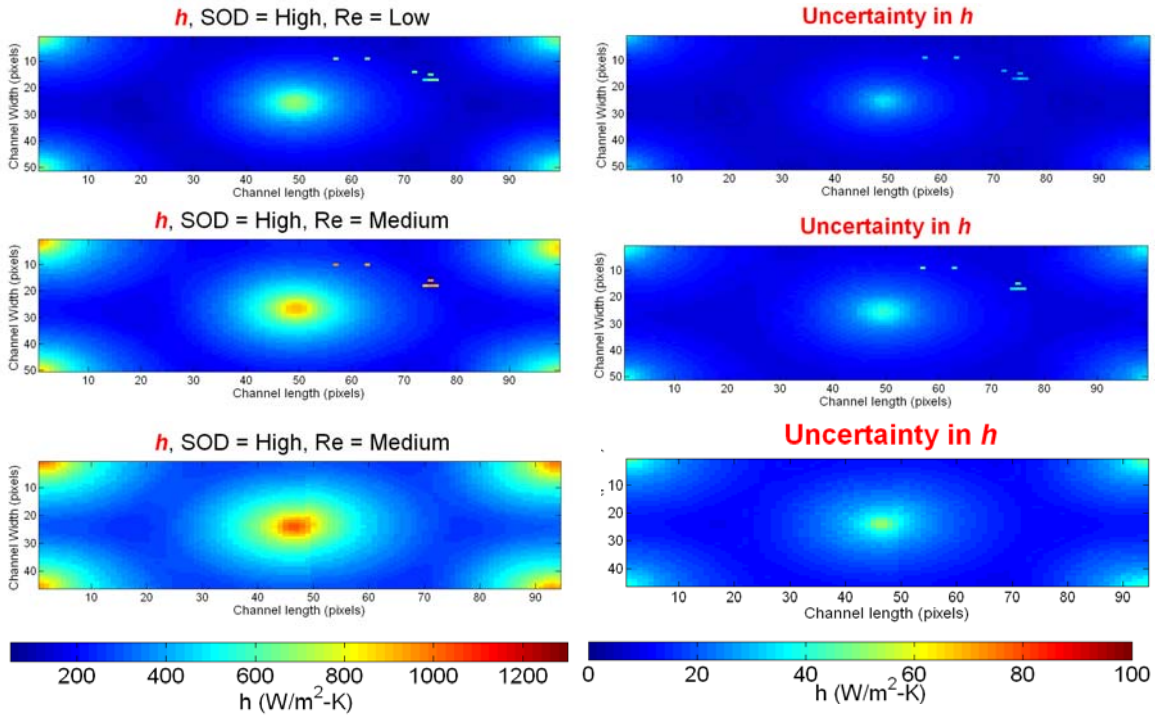

Figure 4.2.2.12 – Heat transfer distributions with associated uncertainty maps for varying flow conditions tested for SOD High. Note: color scale is common between ***h*** maps and Uncertainty in ***h*** maps, respectively.

The three Reynolds number cases for the High SOD case are presented in Figure 4.2.2.12. These results reveal the expected increasing trend with increasing Reynolds number. The higher Reynolds number case, in agreement with the results for Low and Medium SOD cases, reveal the best distribution in heat transfer coefficient overall.

Channels with flow-modifying features

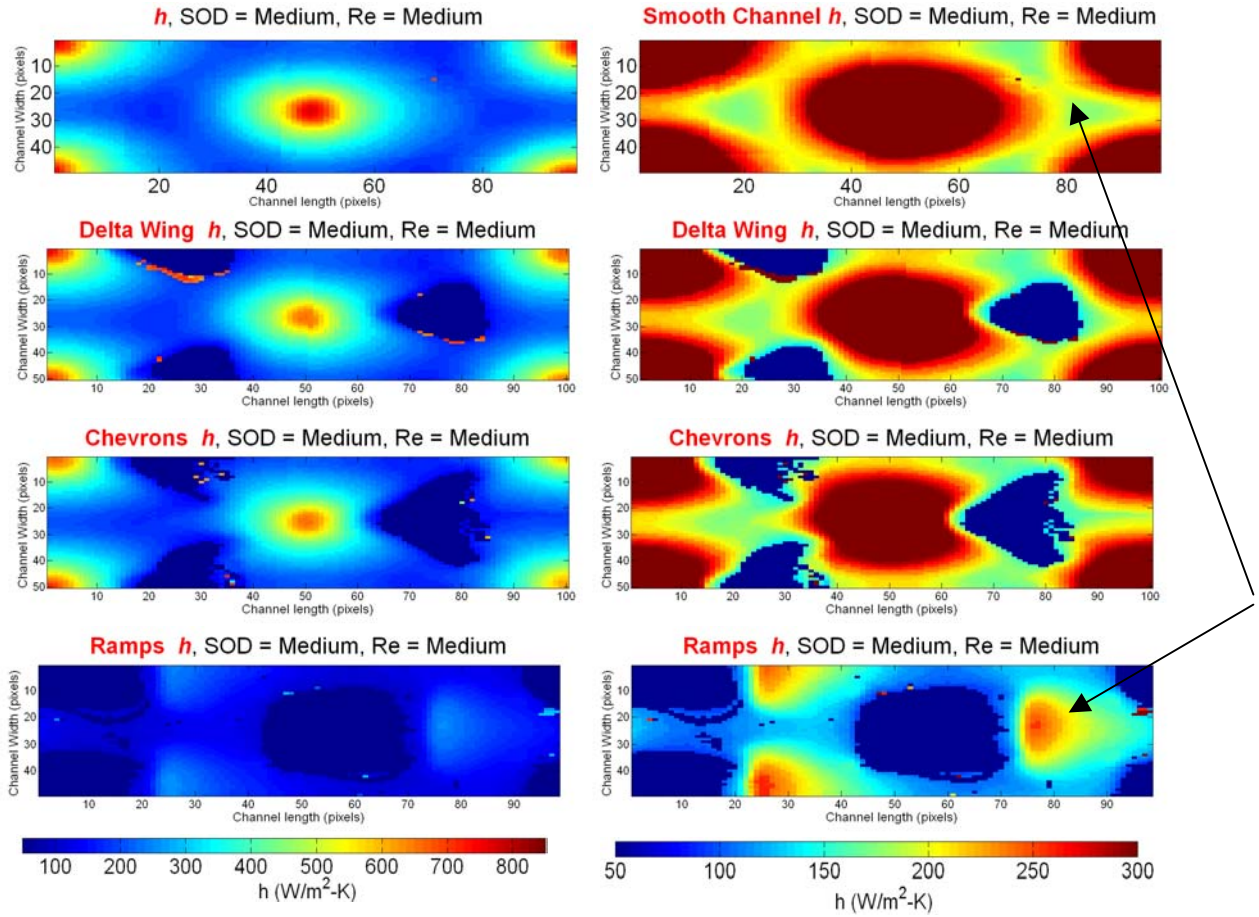

Figure 4.2.2.13 – Heat transfer distributions for three flow-modifying geometries for Medium SOD case, compared with Smooth Channel case. Note: color scale is common for all maps plotted on the left side and all right side, respectively, in order to discern potential benefits in high and low heat transfer regions.

The heat transfer coefficient distributions for the three flow-modifying features are presented in Figure 4.2.2.13 and are plotted along with the smooth channel case at similar Reynolds number and pressure ratio conditions. The data maps are repeated on the right side with the color scale focused in on the data at the lower heat transfer coefficient values in order to discern any difference in the regions of low heat transfer coefficient between the jets. The two turbulating features tested, the delta wings and the chevrons, did not show any significant improvement in heat transfer in comparison to the smooth channel case with no features. The ramp features, which were placed under the jet, revealed good heat transfer enhancement in the downstream region of the ramp. This agrees with the CFD, reinforcing the benefits for ramps in order to redirect the high momentum impingement flow down onto the downstream surface.

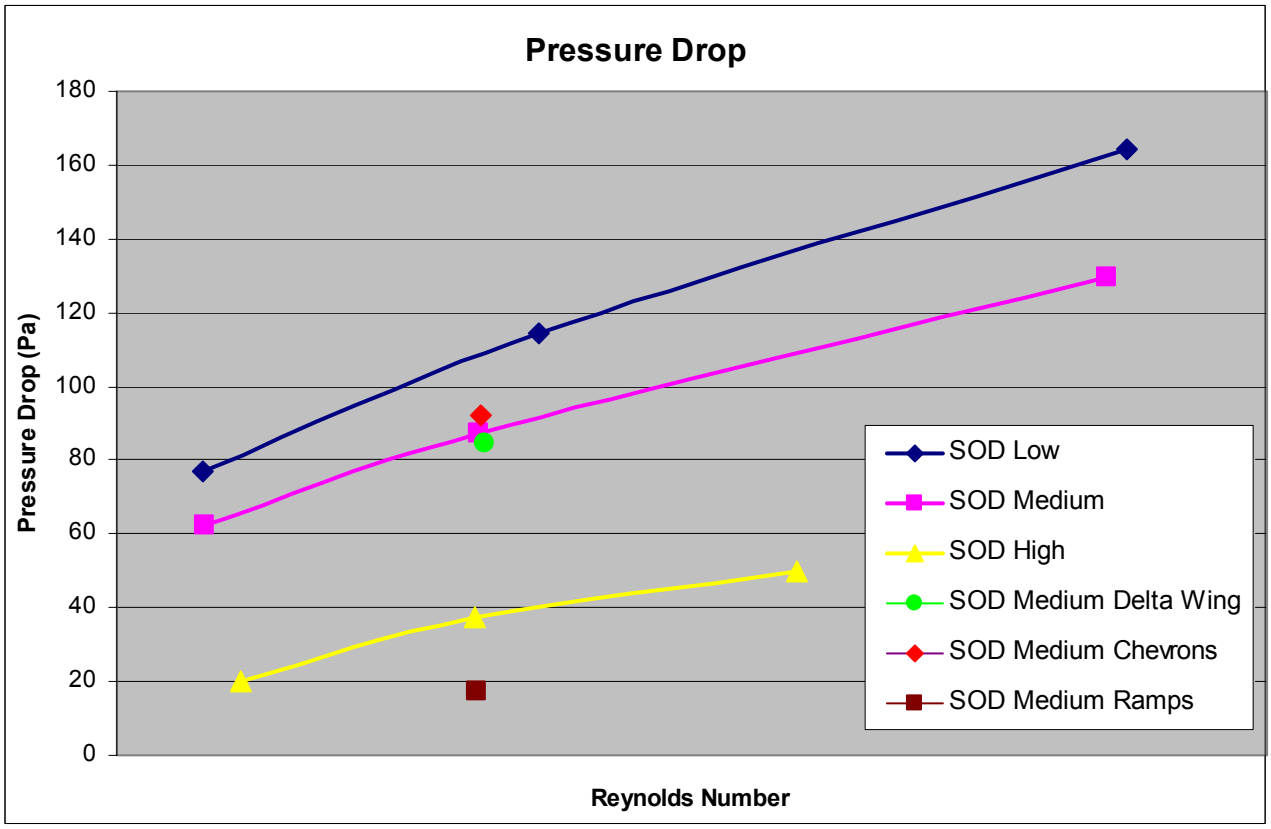

Figure 4.2.2.13 – Pressure drop measurements for different test conditions and SODs tested.

Pressure measurements made with a Monometer are presented in Figure 4.2.2.13. The pressure drop measured across the region of comparison, described in the Technical Approach section, was quite small, lower than 200Pa. The plots reveal an increasing trend in pressure drop with increasing Reynolds number as well as with decreasing SOD. The ramps showed considerably lower pressure drop than the baseline and the two other flow-modifying feature cases. The baseline, the delta wing and the chevron cases all showed very similar pressure drop for the similar test conditions.

Conclusions

The experimental effort generated a good set of impingement flow data for unconfounded matching parameters of interest. These data sets can be used for improving correlations and validating CFD. Three geometries were investigated in combination with impinging flow for potential heat transfer benefits by modifying the flow mechanism in the channel. The results from the ramp features showed potential for better distribution of the cooling air with lower pressure drop, while the delta wing and the chevrons did not show any significant improvement. However, it should be noted that the added surface area by the flow-modifying features for similar pressure drops and similar heat transfer coefficient signatures could potentially lead to gains over the no feature baseline case.

The equipment designed and built for these experiments along with the measurement techniques used show great potential for further investigation of varying features that could result in performance enhancement. The authors already have some features in mind that are worth investigating.

Task 4.2.3 CFD Modeling and Optimization

Subtask 4.2.3.2 Advanced Turbine Blade Cooling

Background

To support the development of the next generation of turbine blade cooling technologies, optimization techniques are needed that allow the timely and efficient screening of blade cooling designs. This requires a coupled design system that rapidly estimates cooling flows, metal temperatures, and blade stresses for candidate designs, and provides multiple levels of optimization.

Objectives

The objectives of this task are to explore the use of optimization techniques applied to turbine blade cooling designs at the 1D, 2D and 3D levels, and develop an integrated design system/optimization tool that can be utilized for the efficient design of cooled turbine blades. The toolset must allow the user to balance the speed of the 1D methodology with the accuracy of the 2D and 3D methods, taking full advantage of the strengths of each level of analysis. Finally, the separate components of the toolset must be integrated to work together, providing efficient through-flow of information between the components.

Technical Approach

Several new tools have been developed throughout this program, collectively known as the Turbine Blade Design System (TBDS). The development of the TBDS system included the construction of the 1D, 2D and 3D Excel based toolsets, and also includes extensive use of the ANSYS commercial software package. The three-level suite of tools has been established to provide rapid screening of potential cooling configurations (1D analyses) while improving the accuracy to which the design constraints are evaluated (2D and 3D analyses).

The 1D design tool models the airfoil as a series of panels with a prescribed wall thickness, and the cooling air as a 1D flow circuit. For a given geometry, the flow solution and 1D thermal solution at each panel is solved simultaneously. Use of the 1D method allows quicker screening of the general cooling configuration at the beginning of the design process. Since the entire system is contained within Excel, DOE and optimization techniques can be employed to evaluate a large number of configurations and identify the basic design space that will satisfy the cooling needs of the blade.

Once design candidates are selected from the design space, the flow geometric inputs, external boundary condition tables, and flow solutions can be handed off to the 2D TBDS design system. The improved accuracy of the 2D thermal results allows the user to refine the design space and is used for additional optimization based on thermal and stress constraints.

After the 2D optimization is complete, the internal flow geometry, flow solution, and external boundary condition tables are passed to the 3D TBDS design system to evaluate the 3D stresses and thermal results, and provide the final level of optimization.

The end result is a three-level system (1D, 2D, and 3D) that functions together to produce a screening/design/optimization environment for cooled turbine blades. With these tools, the user can evaluate many internal cooling configurations to find a design that best meets the thermal, stress, and flow requirements of a given system. The following sections describe the technical approach utilized for each level of analysis and optimization.

1D TBDS Overview

The 1D thermal analysis system is an Excel-based modeling environment designed as a rapid screening tool for basic cooling configurations of a turbine blade. The system splits the exterior of the blade into a number of panels and calculates the temperature on the inside and outside of the panel using a 1D thermal resistance network. The tool also contains a simplified network flow solver, to provide internal boundary conditions for the thermal solver. The resulting film temperatures are combined with the uncooled gas path data to develop the external boundary conditions. The flow network solution is iterated with the 1D thermal solution at each panel until a consistent thermal/flow solution is reached for all of the panels. The 1D TBDS analysis system has the ability to:

- Solve 1D network solution based on user supplied chamber/element data
- Calculate external thermal BC's (HTC and film temperature) based upon the uncooled gas path data, 1D cooling flow solution, and user input film effectiveness curves.
- Calculate the internal thermal BC's using the 1D flow solution and user supplied correlations.
- Calculate panel surface temperatures
- Calculate cooling air heat pickup
- Reduce standard deviation of metal temperature by varying any of the geometric variables (e.g. hole sizes, numbers, spacing, location, etc.).

Uses of the tool include determining film requirements, flow splits, and backside cooling levels that are needed to reach target metal temperatures at each panel. 2D heat conduction to the blade interior, and thermal stress is not considered at the 1D TBDS level.

1D Thermal Analysis Methodology

The thermal analysis method used to calculate metal temperatures is based upon a thermal resistance calculation. The panel is modeled with a gas path temperature, backside cooling air temperature, and TBC and metal thickness, as shown in Figure 4.2.3.2.2. Internal HTCs are determined from the current 1D flow solution, the geometric inputs for each panel, and convection correlations. Using the calculated HTC, the size of the panel, and the incoming flow, the heat flux is computed and added to the flow. Any resulting film from a panel is combined with the external uncooled airfoil solution to estimate the film temperature and

HTC on the external surface; film accumulation effects are included. The total heat flux through the system is then calculated using the resistance network in Figure 4.2.3.2.2. This process results in a coupled solution of the 1D temperature distribution for each panel, and cooling circuit flow rates, pressures, and temperatures throughout the cooling circuit.

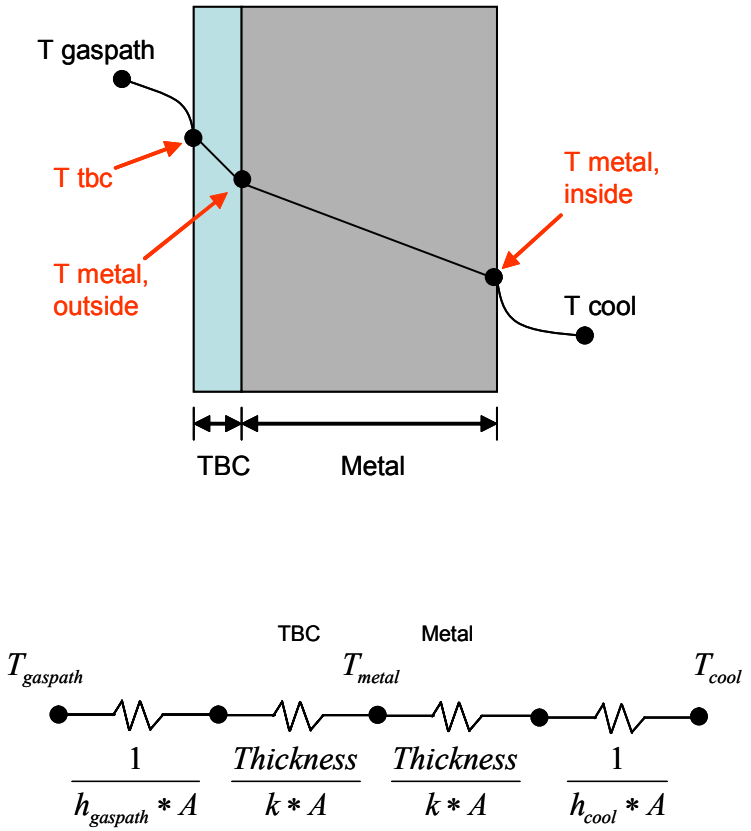

Figure 4.2.3.2.2 Schematic of 1D thermal solver

1D Flow Network Methodology

A 1D flow network solver has been developed for use in the TBDS system. The flow network is used to calculate flow rates and pressures for the internal cooling network at three span wise locations: 15%, 50%, and 85% span. However, the 1D TBDS only utilizes the results at the 50% span. Pressure drops due to constrictions are calculated, as are vortex pumping effects. Development of the 1D solver allows the solution to be completed in Excel, providing efficient integration with the 1D thermal analysis. Currently, the solver can handle simple orifice elements, fixed flow elements, vortex pumping, momentum chambers, but does incorporate tube elements.

2D TBDS Overview

The 2D design system utilizes the basic geometric inputs and flow solution from the 1D tool, along with the external uncooled boundary conditions and film effectiveness curves. The 2D tool combines the data from the 1D tool with a solid model of the actual geometry and ANSYS scripts for automated mesh generation and model control. The solid model represents the 50%-pitchline geometry extruded in both directions to get 20% of the total height. The TBDS spreadsheet obtains additional geometry information of the blade design from the solid model and the engineer. At this point, the TBDS writes all input files for the ANSYS model at the pitch line. An ANSYS script written with the input files, and several ANSYS subroutines complete the thermal model for the given design.

The script executes the solution by first determining the HTC's on all internal cavity surfaces. The HTC's are determined from a combination of the flow solution and several subroutines that mimic standard correlations.

To couple the internal and external cooling components, the mapped external boundary conditions are modified to account for film cooling in a manner identical to the 1D tool. The film hole exit temperature is then used as the supply air for the external film cooling.

The final temperature exiting the film row is used to film the outside blade surface. The new film temperature form the final external boundary conditions for the thermal analysis.

Within the TBDS package, a DOE matrix can be set up to evaluate any number of parametric geometric variations. The DOE matrix of runs is included in the control scripts output by the TBDS spreadsheet, and the variables are automatically sequenced to produce solution sets for each case. The results can then be analyzed through a neural network system to evaluate the design space.

3D TBDS Overview

The 3D design system utilizes the same process as the 2D model, except now the blade model starts at 0% span and goes to 90% span. The model is constructed by lofting the blade between the 0% and 50% cross-sections and then between the 50% and 85% span cross sections. The 3D model also differs from the 2D model because the blade is then split into 3 segments. Essentially, three independent segment calculations are performed with the coupled internal and external boundary conditions for each of the three segments, in a process identical to the 2D TBDS model. The 3D model approach will be discussed in further detail next.

The 3D TBDS system starts by constructing a solid model of the full airfoil height of the blade. The 3D airfoil solid model is constructed by lofting three sections at the hub, pitch and tip. The solid model is then exported for finite element meshing

Similar to the 2D TBDS model, the flow solution from the 1D TBDS system can be utilized for the 3D model, or an new flow solution can be developed based on the 3D thermal solution.

An automated mesh generation procedure has been scripted to import the geometry and construct a tetrahedral mesh for the finite element analysis. The blade metal and thermal barrier coating (TBC) volumes are both meshed with tetrahedral elements.

The external boundary condition requirements for the thermal analysis are identical to the 1D and 2D TBDS requirements. These data can be calculated using the same procedure as the 1D and 2D models, or from a mapping of a detailed 3D CFD analysis of the blade.

For the internal heat transfer conditions, the flow network solution and turbulent boundary layer correlations were used to set the heat transfer coefficients on faces cooled convectively. Correlations were also used to determine the local enhancement due to wall roughness or turbulators. Impingement correlations were used to determine HTC's on impinged faces, again using the flow network solution for flow rate and pressure ratio.

Air temperatures for the internal thermal boundary conditions are solved concurrently with the metal, to account for heat pickup in upstream elements of the flow circuit.

The 3D TBDS tool includes the effect of the film row bore cooling using the 2D TBDS methodology extended to the full span, by defining a strip of elements along the path of the film holes from hub to shroud, through the wall thickness.

The ANSYS model incorporates an internal advection network that estimates the coolant heat pickup based on the current metal temperatures, and the script ties the different legs of the circuit together

The same mesh is used for the mechanical analysis as was used for the thermal analysis. The blade platform connection is modeled using constraints; the entire inner surface is

constrained to a constant radius. One point on the trailing edge is further constrained in both z and theta to prevent translations, and a point near the suction side maximum curvature location is constrained tangentially to prevent rotations. The previous thermal results are applied as temperature loads, and the blade rotation is included to superimpose the inertial load on the thermal load.

Optimization Technique

The optimization techniques used in the current study were twofold. The first level of optimization was completed at the 1D level, and focused primarily on setting the impingement hole sizes and film row locations. The first step was to run the 1D model for a number of film row flow areas at varying distances from the leading edge. The results were processed through a neural network to minimize the metal temperature variation at each panel and the peak metal temperature at any panel.

The resulting flow solution and circuit geometry were saved for each case, and handed off to the 2D TBDS system.

Each of these runs was then analyzed with the 2D TBDS model, to generate accurate metal temperature results. These results were used to train a neural network to optimize the overall mass flow rate based on peak metal temperature.

Although the 2D stresses were calculated as part of the 2D TBDS analysis, they were not directly used for the optimization. This was because the 2D thermal stresses were found to be an insufficient indicator towards the overall blade stresses. The calculated stresses could be used as part of the optimization to minimize the calculated stresses, but the value would be very limited. The final optimized solution was passed through the 3D TBDS system to evaluate the 3D temperature and stress results. However, no further optimization was completed at the 3D level.

Results

Baseline Turbine Blade

A typical serpentine geometry was run through the 2D TBDS system previously described to provide a baseline.

The first step in the setup of the analysis was to incorporate the internal flow solution of the serpentine model into the TBDS spreadsheet. The spreadsheet was used to setup the inputs for the ANSYS thermal/stress analysis. The TIP/film hole, cavity geometry, source pressure and temperature data are incorporated into the spreadsheet.

Optimized Turbine Blade Design

For the optimization process, no surface enhancement was utilized. The results found in the current study could be improved upon with the use of surface enhancement. Also not considered were design constraints based on manufacturing limitations. For actual design optimizations additional constraints would have to be applied.

2D Optimization Results

In order to determine a feasible flow solution, both the 1D and 2D optimization techniques were utilized. The 1D TBDS system was exercised first, to optimize the film row location that provided the best coverage for the airfoil. The film row locations were then frozen, and the 1D system used to solve 130 data sets.

The flow solutions and geometry for each case were loaded into the TBDS spreadsheet and 2D thermal models were completed for each case. Using the 2D thermal results for each case, a neural network was trained based on the 11 input variables (individual film row flow rates). The trained neural network was then used to predict output parameters for ~65,000 cases. The selected output parameters for the training were the max surface temperature and the standard deviation of the surface temperatures. The goal was to determine which combination of flow splits used the lowest amount of flow to yield a flat and smooth surface temperature at or below a maximum surface temperature.

The neural network predicted results were then filtered based on the lowest total flow rate with the lowest max temperature and standard deviation. Six cases were selected as the best solutions. These six cases were then verified by analyzing them with the 2D TBDS system. The neural network predicted values of the standard deviation were within ten percent of the actual standard deviation for all but one case. The max surface temperatures were predicted to within five percent of the actual values. One of two approaches could be taken at this point: the first approach would involve narrowing the input parameter values based on these results in an effort to zero in on the optimum flow configuration, or one of the six cases could be selected to be the representative optimized solution. Using the latter approach, case number 134 was selected as the best case, based on having the highest flow reduction with the maximum surface temperature closest to the target cutoff.

Total flow was reduced by 10%. As expected, the reduction in flow and subsequently the increase in surface temperatures resulted in increased stress levels, especially in first principle stress. An optimization involving the cavity geometry and the stress levels would need to be completed in order to reduce the stress levels to acceptable ranges. However, the current study will show that the 2D stresses are not sufficient to properly evaluate the design of the turbine blade. 3D analysis is required to optimize the design for stresses.

3D Model Results

The 2D optimized case was now taken into the 3D modeling system. A full thermal solution and stress analysis was completed. Comparing the temperature contours of the 3D model to the 2D model, the results compare very well, however the 3D results are generally higher. Since the optimization effort has not involved the trailing edge, the specific reasons for the differences at the trailing edge will not be examined here.

As expected, the 3D stresses are very different from those found in the 2D solutions. The radial stresses are the dominant stress field for the turbine blade, as a result of both the inertial forces and the thermal stress induced by the temperature difference between the interior and exterior of the blade. This is why the stresses cannot be sufficiently optimized at the 2D level. The 3D modeling techniques used in the current stress analysis has been simplified compared to a detailed stress model, in an attempt to automate model construction and reduce overall process time. Including more geometric details should improve the stress results, but the impact on the calculated values is unknown.

Conclusions

A 3 level tool for the design and optimization of turbine blades has been developed. The 1D TBDS system utilizes EXCEL macros to provide optimization of the basic cooling configuration chosen, and can automatically redistribute the flow to reduce the temperature gradient around the airfoil. The 2D TBDS system is then employed through EXCEL macros to efficiently analyze a large number of cases through ANSYS. 2D analysis has proven sufficient to optimize the flow distribution to minimize the metal temperature and overall flow rate. As part of the system, numerous ANSYS macros were also developed to facilitate the construction of the models, and to interface with the EXCEL outputs. Finally the 3D TBDS system allows the user to take a design from the 2D TBDS spreadsheet, and rapidly complete a 3D ANSYS thermal and stress analysis on a simplified 3D blade. The 3D analyses are required to properly analyze the stress field of the turbine blade. For a given flow distribution the 3D system can be used to evaluate the stress fields for multiple geometries. These results can then be used to train a neural network and generate an optimized solution for reduced stresses.

Subtask 4.2.3.3 Cooling Feature Optimization

Background

Impingement cooling is extensively used in gas turbine cooling applications especially to cool the high pressure turbine blade leading edges, where high heat load is experienced from flow stagnation. In an effort to supplement the TBDS development package developed under the current program, a computational fluid dynamic (CFD) study is undertaken to look at ways of enhancing the impingement heat transfer for sparse array cooling applications.

Technical Approach

A baseline CFD model was created with a jet-to-wall spacing of 4D (D=circular hole diameter=0.030") and square array with hole spacing of 15D. Due to the flow symmetry between adjacent holes in the array, it is sufficient in CFD to model the region around a single hole (Fig. 4.2.3.3.1b). To prevent the exit boundary from influencing (flow into and out of the domain) the impingement region of interest, an extension is added

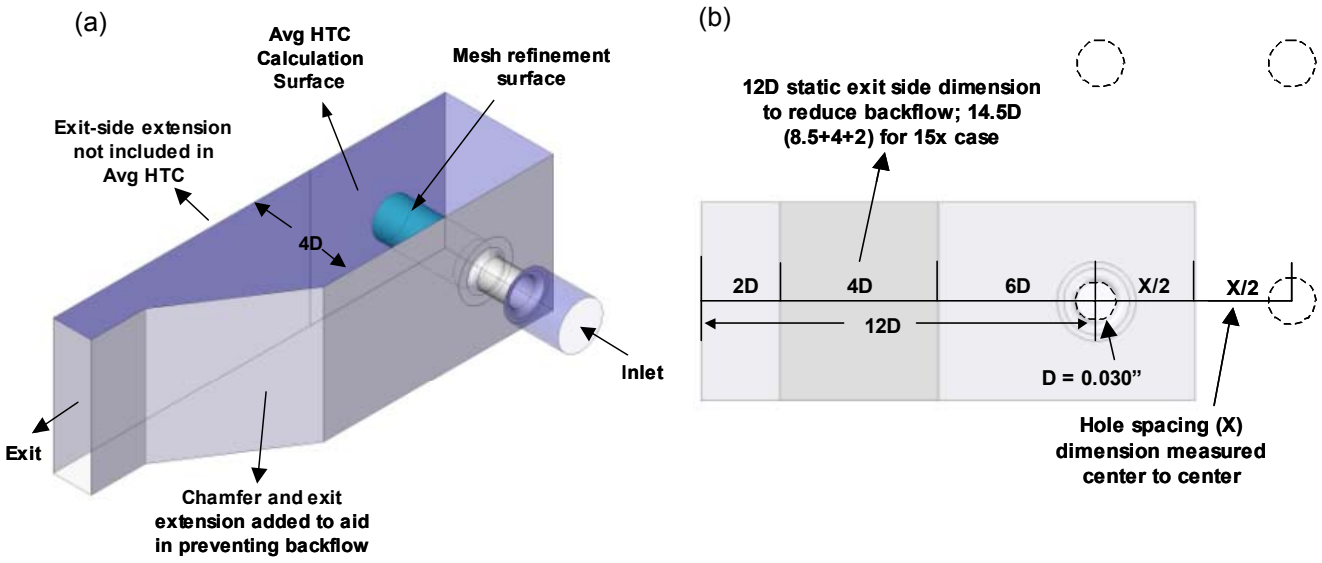

Figure 4.2.3.3.1: (a) – CFD domain setup (b) – CFD domain (in grey) position in

CFD meshes were built to be hybrid with prisms to resolve the boundary layer and tetrahedral mesh in the far field. The first cell spacing from the impingement wall is set to achieve y+<5. CFX10 was used as the flow solver. The CFD models were solved in the stationary frame with the K-Omega turbulence model.

Results

CFD was used to evaluate techniques of increasing the heat transfer effectiveness in sparse array cooling applications. Several parameters were examined.

Conclusion

A CFD study was undertaken to increase the impingement heat transfer effectiveness in sparse array cooling applications. The baseline CFD model was validated against Kercher's array impingement correlation. Further studies are needed to understand and design an advanced impingement array.

REPORT DOCUMENTATION PAGE	Form Approved OMB No. 0704-0188

1. REPORT DATE *(DD-MM-YYYY)*	2. REPORT TYPE	3. DATES COVERED *(From - To)*
01-06-2008	Final Contractor Report	July 2006-July 2007

4. TITLE AND SUBTITLE
Intelligent Engine Systems
Thermal Management and Advanced Cooling

5a. CONTRACT NUMBER
NAS3-01135

5b. GRANT NUMBER

5c. PROGRAM ELEMENT NUMBER
4.2

6. AUTHOR(S)
Bergholz, Robert

5d. PROJECT NUMBER

5e. TASK NUMBER
37

5f. WORK UNIT NUMBER
WBS 984754.02.07.03.11.03

7. PERFORMING ORGANIZATION NAME(S) AND ADDRESS(ES)
General Electric Aircraft Engines
One Neumann Way
Cincinnati, Ohio 45215

8. PERFORMING ORGANIZATION REPORT NUMBER
E-16495

9. SPONSORING/MONITORING AGENCY NAME(S) AND ADDRESS(ES)
National Aeronautics and Space Administration
Washington, DC 20546-0001

10. SPONSORING/MONITORS ACRONYM(S)
NASA

11. SPONSORING/MONITORING REPORT NUMBER
NASA/CR-2008-215236

12. DISTRIBUTION/AVAILABILITY STATEMENT
Unclassified-Unlimited
Subject Category: 07
Available electronically at http://gltrs.grc.nasa.gov
This publication is available from the NASA Center for AeroSpace Information, 301-621-0390

13. SUPPLEMENTARY NOTES

14. ABSTRACT
The objective is to provide turbine-cooling technologies to meet Propulsion 21 goals related to engine fuel burn, emissions, safety, and reliability. Specifically, the GE Aviation (GEA) Advanced Turbine Cooling and Thermal Management program seeks to develop advanced cooling and flow distribution methods for HP turbines, while achieving a substantial reduction in total cooling flow and assuring acceptable turbine component safety and reliability. Enhanced cooling techniques, such as fluidic devices, controlled-vortex cooling, and directed impingement jets, offer the opportunity to incorporate both active and passive schemes. Coolant heat transfer enhancement also can be achieved from advanced designs that incorporate multi-disciplinary optimization of external film and internal cooling passage geometry.

15. SUBJECT TERMS
Gas turbine engines; Turbine cooling; Thermal management

16. SECURITY CLASSIFICATION OF:			17. LIMITATION OF ABSTRACT	18. NUMBER OF PAGES	19a. NAME OF RESPONSIBLE PERSON
a. REPORT	b. ABSTRACT	c. THIS PAGE			STI Help Desk (email:help@sti.nasa.gov)
U	U	U	UU	56	19b. TELEPHONE NUMBER *(include area code)* 301-621-0390